Climate archives from a Viking Age site, Scotland: Seasonal temperature variability during the Medieval Warm Period

Michael Philip Mobilia

A thesis submitted to the faculty of the University of North Carolina at Chapel Hill in partial fulfillment of the requirements for the degree of Master of Science in the Department of Geological Sciences

Chapel Hill
2009

Approved by:

Advisor: Dr. Donna M. Surge

Reader: Dr. Jonathan M. Lees

Reader: Dr. Laurie C. Steponaitis

ABSTRACT

Michael Philip Mobilia: Climate archives from a Viking Age site, Scotland: Seasonal temperature variability during the Medieval Warm Period
(Under the direction of Donna M. Surge)

The Medieval Warm Period (MWP; 800-1300 AD) represents a recent period of warm climate that can be compared to today's warming trend. However, the spatial and temporal variability inherent in the MWP makes it difficult to differentiate between global climate trends and regional variability. Acquiring high-resolution temperature data from this period will allow for increased understanding of temperature variability during this climate interval.

We used oxygen isotope ratios preserved in archaeological limpet shells (*Patella vulgata*) collected from Viking aged midden deposits as a proxy for sea surface temperature. Samples were micromilled to achieve submonthly resolution. Summer and winter temperatures averaged $13.4 \pm 0.7^{o}C$ and $5.9 \pm 0.8^{o}C$, respectively. When compared to regional data from NOAA ($12.40 \pm 0.39^{o}C$ and $7.76 \pm 0.44^{o}C$) from 1961-1990, MWP summer temperatures were warmer than current averages, and winter temperatures were cooler. Our results indicate that MWP seasonality was greater than that observed today.

ACKNOWLEDGEMENTS

I would like to thank Dr. Donna Surge for her support and guidance during this project. She created a great project, and I wouldn't have been able to finish it without her help. This project generated some really interesting results, and it and all future projects (of which there are many I'm sure) are all due to Donna's insight and great motivation.

I would also like to extend my thanks to my committee members, Dr. Jonathan Lees and Dr. Laurie Steponaitis. They were both a great help. Additionally, I would like to thank the other members of our lab group: Joel Hudley, Dr. Jose Rafa Garcia-March, and Ting Wang. They were always available and willing to help me out when I needed it. Thanks also to Dr. James Barrett, who was a tremendous resource while I was in the Orkney Islands; I would not have had nearly as productive a trip without his assistance. I also want to thank Anne Brundle and the Orkney Museum for letting me use their shells.

I would like to thank my undergraduate advisor, Dr. Hiroshi Ohmoto. His guidance as I was just starting to study geology was invaluable; he made me a better scientist. I would like to especially thank the friends at UNC that I have made during this process. They made this experience truly great. Finally, thanks to my family for their love and support.

TABLE OF CONTENTS

LIST OF TABLES

LIST OF FIGURES

LIST OF ABBREVIATIONS AND SYMBOLS

α	fractionation factor between calcium carbonate and water
AD	Anno Domini
$59^{o}24'N$	59 degrees, 24 minutes North
^{o}C	degrees Celsius
$\delta^{13}C$	carbon isotope ratio
$\delta^{18}O$	oxygen isotope ratio
DIC	dissolved inorganic carbon
e.g.,	for example
et al.	and others
etc.	et cetera
g	gram
i.e.,	that is
IPCC	Intergovernmental Panel on Climate Change
m	meters
µm	microns or micrometers
µg	micrograms
mm	millimeter
MP	megapixel
MWP	Medieval Warm Period
NAO	North Atlantic Oscillation
NBS	National Bureau of Standards

NOAA	National Oceanic and Atmospheric Administration
P. vulgata	*Patella vulgata*
1σ	one sigma range
‰	per mil or parts per thousand
±	plus or minus
psu	practical salinity units
SST	sea surface temperature
T	temperature
VPDB	Vienna Pee Dee Belemnite
VSMOW	Vienna Standard Mean Ocean Water
YBP	years before present

CHAPTER 1

CLIMATE ARCHIVES FROM A VIKING AGE SITE, SCOTLAND: SEASONAL TEMPERATURE VARIABILITY DURING THE MEDIEVAL WARM PERIOD

Michael Mobilia

Department of Geological Sciences, University of North Carolina at Chapel Hill, Chapel Hill, NC 27599, USA, email: mobilia@email.unc.edu

Introduction

Anthropogenic forcing continues to change our current climate, increasing the necessity for accurate predictions of the scope and timing of future climatic changes. The study of paleoclimate is vital in gaining this understanding, as it allows us to observe how climate has behaved in the past. The late Holocene (~3000 YBP to present) has been identified as an ideal period for study, as it offers the chance to evaluate not only climatic changes, but also human-climate interactions. We chose to study the Medieval Warm Period (700-1100 YBP), as it represents a relatively recent period of a warm climate and, as such, provides an interesting comparison to today's continuing warming trend. However, the Medieval Warm Period exhibits spatial and temporal variations in temperature that make it difficult to differentiate between global climate trends and regional variability [Hughs and Diaz, 1994; Mann and Jones, 2003; Brazdil et al., 2005; Jansen et al., 2007; and others]. Continued study of the period will allow for the analysis of data from a wider geographical range, providing a more accurate picture of regional and global variability during this time.

The study of coastal environments is especially important, as coastal regions are extremely vulnerable to changing climate conditions. Small changes in temperature have been shown to cause significant changes in the ecology of near-shore environments [Taylor, 1995], suggesting that future warming may result in large-scale ecological changes. The effects of climate change on coastal areas can also have serious societal impacts. At present, a large percentage of the world's population lives within 100

kilometers of coastlines and 200 meters of sea level [Cohen, 1997; Small, 2004], and is at risk from the consequences of climate change.

The use of shells as a proxy for marine and coastal climate offers a counterpart to the large number of paleoclimate archives obtained from either deep marine or arctic environments and is important in further reinforcing our knowledge of coastal climate [Dansgaard et al., 1984; Alley, 2000; D'Arrigo et al., 2006; Stott et al., 2009]. Coastal archaeological deposits can provide a rich resource of paleoclimate archives for such environments. Past coastal societies obtained much of their sustenance from the ocean; consequently, there are often a large amount of shells found in archaeological middens. The use of mollusc shells as a proxy for temperature has been well-documented [Epstein et al., 1951; Williams et al., 1982; Jones, 1983; Jones and Quitmyer, 1996; Surge and Walker, 2005, 2006], so the abundance of archaeological shell deposits provides ample opportunity for paleoclimate study. Not only can these shells serve as paleoenvironmental archives, but they also offer a unique opportunity to study the relationships between past human societies and climate [Shackleton, 1973; Walker and Surge, 2006].

We sampled shells of the European limpet, *Patella vulgata*, obtained from a Viking age site in the Orkney Islands, Scotland to test the hypothesis that climate during the Medieval Warm Period exhibited higher temperatures and decreased seasonality compared to today. This was accomplished by analyzing oxygen isotope ratios ($\delta^{18}O$) of shell carbonate as a proxy for sea surface temperature.

Ecology of *Patella vulgata*

P. vulgata is a gastropod inhabiting rocky shorelines in the cold- and warm-temperate biogeographic provinces from Norway to Spain. Prior studies record that *P. vulgata* lives in water with salinities ranging from 20 to 35 psu (practical salinity units) and temperatures ranging from -8.7 to 42.8^{o}C [Crisp, 1965; Branch, 1981]. *P. vulgata* lives on a home base or scar, and only ventures short distances to forage for algae, diatoms, and spores; consequently, the shell records environmental conditions from a single location.

P. vulgata from the United Kingdom differs from other *Patella* species found farther to the south in that it slows its growth during the winter, with maximum growth occurring during the summer months [Lewis and Bowman, 1975; Ekaratne and Crisp, 1982; Jenkins and Hartnoll, 2001; Schifano and Censi, 1986]. Growth rates range from approximately 0.005 mm/month to 2.6 mm/month [Ekaratne and Crisp, 1984].

The shell of *P. vulgata* is conical and averages 6 cm in length, with the apex central or slightly anterior. The outer surface can exhibit coarse radiating ridges and visible growth lines. In cross section, shells exhibit both major and minor growth lines. Major growth lines are annual and formed during the winter in individuals collected from the United Kingdom [Fenger et al., 2007]. They signify a slow down in growth rate during winter months, most likely due to temperature and reproductive processes [Bourget, 1980]. Minor growth lines are observed in bundles of approximately 14 to 15

growth increments. This suggests the minor growth increments represent fortnightly time intervals, composed of microgrowth increments controlled by tidal cycles.

Study Area

Our study area is located on the isle of Westray in the Orkney Islands (Figure 1). The Orkneys (59°24'N, 2°22'W) comprise an archipelago to the north of Scotland and are mostly of low relief. They lie within the cold temperate biogeographic province, yet the influence of the nearby Gulf Stream results in a relatively mild climate. Winter sea surface temperatures average 7.76 °C ± 0.44°C and summers average 12.40 °C ± 0.39°C (Figure 2; monthly averages, from NOAA SST reconstruction 1961-1990). The proximity of our site to both the Gulf Stream and the North Atlantic Oscillation make it an extremely interesting location to study Medieval Warm Period climate.

Samples were obtained from the Viking village of Quoygrew, situated on the coast of the large northwest-facing Rackwick Bay. The village of Quoygrew is a well-preserved rural settlement occupied from the Viking Age to post-medieval times. Shells collected from Quoygrew will serve as an archive of sea surface temperature adjacent to the site, and by extension, help characterize the climate in the North Atlantic.

Local Climate Mechanisms

The North Atlantic Oscillation (NAO) and the Gulf Stream both play major roles

in the climate of northern Europe. Consequently understanding these climate mechanisms is vital to the study of Medieval Warm Period climate. The location of the Orkney Islands places them in a region influenced both by the NAO and the Gulf Stream, so temperature data collected from our field site in Orkney may potentially offer insight as to the state of these climate mechanisms during the interval of study.

Today, both the Gulf Stream and the NAO are widely recognized as the major sources for short-term climate variability in the North Atlantic realm. The NAO alone is responsible for 31 percent of interannual temperature variance in the North Atlantic – NW Europe region [Hurrell and van Loon, 1997]. In addition to variability induced by the NAO, the influence of the Gulf Stream is thought to affect precipitation and atmospheric circulation changes throughout the entire troposphere [Minobe et al., 2008]. When teleconnections between the NAO and the Gulf Stream are taken into account, these two climate phenomena potentially have a large influence on the climate of the North Atlantic.

Gulf Stream

The Gulf Stream is the northward flowing western boundary current associated with the North Atlantic gyre. The climate of Europe is dependent upon the Gulf Stream; thus, disruptions or changes in the activity of the current have large effects on regional climate. Studies by Lund et al. [2006] have shown the Gulf Stream flow density gradient was lower during the Little Ice Age (1650-1850 AD). Coupled with the fact that the

volume transport of the Gulf Stream is thought to have been approximately ten percent weaker during that period, it is likely a weakened Gulf Stream was a contributing factor to the Little Ice Age [Lund et al., 2006]. Knowing this, it is also possible the Medieval Warm Period may have been caused by an increase in heat transport northward, although no conclusive results have yet been produced on this topic.

In addition to large scale variability associated with dramatic changes in thermohaline circulation, the Gulf Stream undergoes higher frequency, smaller scale variability. These changes typically result in latitudinal displacements of the Gulf Stream, with the current migrating north and south aperiodically [de Coetlogon et al., 2006]. Studies of plankton in the North Atlantic have shown changing abundances that can be correlated with the location of the Gulf Stream [Taylor, 1995]; similarly, lakes in the United Kingdom exhibit changes in their chemistry that are in phase with Gulf Stream variability [Jennings and Allot, 2006]. This implies the north-south migration of the Gulf Stream has climatological effects throughout the Atlantic and northern Europe, likely caused by the changing distribution of heat as the Gulf Stream moves. This change in temperature is accompanied by, or perhaps causes, changes in the number of North Atlantic cyclones, another factor that influences northern European climate [Taylor, 1995].

North Atlantic Oscillation

The NAO describes the climatic phenomenon located in the North Atlantic Ocean

characterized by the fluctuations in sea level pressure between the Icelandic Low and the Azores High. The oscillation between these pressure centers results in variations in the strength of the Westerlies over Europe, and is a major source of variability and one of the most important climate mechanisms in the North Atlantic – European region.

The NAO exhibits no obvious periodicity, but instead a mix of different, mostly small-scale periodicities [Cook et al. 2002]. Some variability is also seen on longer, interdecadal timescales, but is poorly understood [Wanner et al., 2001].

During the positive phase of the NAO (NAO+), the strong pressure gradient strengthens the Westerlies and forces them farther to the north. This results in the flow of warm air over much of northern Europe, which increases surface temperatures throughout northern Europe. It also causes a northward shift in Atlantic storm activity, and increases precipitation over affected areas. The resulting effects of a NAO+ would result in regional climate that mirrors what is seen in northern Europe during the Medieval Warm Period. Mann [2007] proposed that the cold continental air mass resultant from a negative phase of the NAO may be directly related to the decreasing temperatures during the span of the Little Ice Age. If this is indeed the case, it is reasonable to assume other climatic episodes (such as the Medieval Warm Period) may be related to changes in the NAO.

During the atmospheric pressure changes associated with the NAO, geostrophic flow in the North Atlantic is affected, which can lead to the north-south oscillations seen

in the location of the Gulf Stream [Taylor and Stephens, 1998]. Positive phases of the NAO have been correlated to a stronger, farther north flowing Gulf Stream, while a negative NAO is generally followed by a weaker, southern flowing Gulf Stream [de Coetlogon et al., 2006]. This has a substantial impact on climate in northern Europe, as the NAO and Gulf Stream can, through this interaction, amplify their effects on the North Atlantic.

To date, knowledge of the Medieval Warm Period suggests a time of inherent variability, with temperatures ranging above the averages of the preceding and subsequent time intervals. Based on our understanding of NAO climatic effects, a period of warm temperature in northern Europe may suggest the existence of a positive phase NAO at this time, as well as a northward-shifted Gulf Stream [Stenseth et al., 2003]. This is contrary to what was seen in the Little Ice Age, during which it is suspected a persistent negative phase NAO, coupled with a decrease in Gulf Stream transport, contributed to colder temperatures [Mann, 2007].

Medieval Warm Period

The Medieval Warm Period is the name given to the climatic episode that occurred in Europe from roughly 900 to 1300 AD, during the historical medieval period. It is thought the average temperatures in Europe during this period represent values higher than those in the preceding Dark Ages Cold Period or later Little Ice Age. Temperatures observed during the Medieval Warm Period are some of the highest seen in

the last millennia [Jansen et al., 2007]. Only current global warming has produced temperatures that are higher. Because the Medieval Warm Period took place before anthropogenic forcing became a significant driver of climate, any climate change during this period is due to natural forcing [Hunt, 2006; Goosse et al., 2006], making this interval ideal for further study.

However, there is no consensus as to the exact dates bounding this period, and it has been established that this time was not, as previously thought, an episode of continuous above-average temperatures, but rather a period of varying warm and cold intervals [Hughes and Diaz, 1994]. Several more recent studies have questioned the accuracy of some of the historical data that forms the basis of the argument for a Medieval Warm Period [Mann and Jones, 2003; Hunt, 2006], and Jones and Mann [2004] have questioned the existence of such a period. Other studies have questioned the extent of any climatic anomaly, in an effort to determine the scale and regional impact of warming [Crowley and Lowery, 2000; Esper et al., 2002; Hughes and Diaz, 1994; D'Arrigo et al., 2006]. Intergovernmental Panel on Climate Change (IPCC) reports on paleoclimate, some of which have focused on the Medieval Warm Period, have identified several concerns regarding the evidence used as a basis for the existence of this period. These include the lack of temporal correspondence between climatic variability in different regions, regional variability, and the fairly small amplitude of the average temperature anomalies in the affected regions [Hunt, 2006]. However, the most recent IPCC report presents temperature reconstructions that show positive anomalies in the northern hemisphere during the time of the Medieval Warm Period.

Lamb [1965] was among the first to propose the idea of a warm period during medieval times. Much of the original data Lamb used to make his claim was obtained through historical climatology. Agriculture was feasible at higher latitudes and altitudes than is currently possible, and several historical records document large crop yields. Vineyards in central Europe are thought to have been cultivated farther north and at higher altitudes (~220m higher above sea level) than they were in the early 20th century. Similarly, the presence of a large number of vineyards in England also implies warmer temperatures and longer growing seasons [Lamb, 1965; Mann, 2002]. Historical records also note the dates of frosts, freezing of bodies of water, and snow cover which indicate that winters during this period were less intense [Mann, 2002].

Observations of settlements in central Norway have shown the migration of many villages and towns approximately 100-200 meters up valleys and hillsides, in areas that would have previously been covered by snow. These villages had been static before this time, and retreated back down the valleys in the 14th century [Lamb, 1965]. The upper limit of forests in the Alps is thought to have been located up to 200 meters higher than the present tree line, with a return to 20th century altitudes between 1300 and 1600 AD. These changes in altitude correspond to an increase in summer temperatures of approximately 1^{o}C compared to present day temperatures [Lamb, 1965].

Analysis of glacial moraines in northern Europe shows there were periods of glacial advances before 900 AD, and after 1250 AD. However, there is a lack of glacial advancement during the period between 900 and 1250. Some areas of the European Alps

actually show evidence of glacial retreat during this period [Hughes and Diaz, 1994]. Grove and Switsur [1994] also used glacial evidence to study the Medieval Warm Period. They identified a glacial phase that preceded the Medieval Warm Period, beginning around 600-800 AD. Coupled with evidence of the beginning of the Little Ice Age at around 1200 AD, their glacial data seem to imply a period of higher temperatures between 800-1200 AD.

Pfister et al. [1998] attempted to reconstruct the winter climate during the Medieval Warm Period. They created a comprehensive compilation of meteorological texts for the medieval period prior to 1300 AD. This information, in conjunction with documentary proxy data (ice, snow, plant activity) was used to reconstruct winter temperatures over western central Europe for a 550 year period. By analyzing anomalous winters (above and below average) on the basis of proxy data for frost, the freezing of bodies of water, duration of snow cover, and atypical seasonal growth of vegetation, they were able to create an index of winter storm severity. They concluded severe winters were weaker and less frequent during the Medieval Warm Period than in the centuries preceding it, and from 1300-1900 AD. From 1180 to 1299 AD, winter temperatures were similar to those seen in the 20th century.

Some of the most compelling evidence for a Medieval Warm Period is the colonization of Greenland and Iceland by Norse settlers. Settlements on Greenland lasted for several centuries, implying the existence of climate conditions suitable for habitation [Ogilvie, 1991].

Historical climate data imply a period of above average temperatures during the Middle Ages, resulting in more widespread farming, an increased frequency of northern settlement, and an effect on trade due to decreased sea ice. Observations of sea ice, growing seasons, areas of settlement, and agriculture suggest a temperature increase of approximately 1-2^{o}C for the years 1000-1200 AD, with a larger temperature anomaly possible in high-latitude areas [Lamb, 1965]. However, information of this kind is not without considerable error, and must be supported by more accurate temperature data. As more research is performed, it becomes clearer the climate of this period cannot be classified as a synchronous, global warming event, but rather as an episode of climatic variability resulting in several phases of increased temperature, with a great deal of temporal and regional variation. It is the focus on constraining the extent and magnitude of any temperature anomalies during this period that is the basis of much of the current research into the Medieval Warm Period.

Archaeological Context

Shells for our study were collected from the Viking site of Quoygrew in the Orkney Islands (Figure 3). The longhouses and associated middens present at the site document a sequence of settlement from the Viking Age to post-Medieval times (950-1930 AD). This includes the Viking to Medieval transition, which is thought to be accompanied by a change in subsistence strategies by both inhabitants of the Orkneys and other northern European peoples. This change is characterized by an intensification in marine resource use, including an increase in fishing during the 11th century, which

continued into the 14th century [Barrett and Richards, 2004]. This intensification can be seen at Quoygrew, and it is theorized that an expansion of fishing may be the cause of the greater number of limpets found in middens, as limpets were used as bait for the cod fishing industry [Milner et al., 2007].

The shell samples used in this study were recovered from two locations: 1) a midden on the seaward side of the structures, known as the 'fish midden,' and 2) an inland 'farm mound' developed due to the superposition of abandoned building ruins and an associated midden (Figure 3).

Methods

Chronostratigraphy

To create a temperature archive for the Medieval Warm Period, it was necessary to select shells that were harvested during that period. This was accomplished by selecting samples from deposits dated and classified by Milner et al. [2007]. The middens at Quoygrew were divided into four phases, numbered 1 through 4, and were dated, using radiometric and artifactual evidence, to the 10th through 13th centuries. Each phase covers a period of approximately one hundred years. The middens are well stratified, and shells taken from the site were cataloged according to phase, allowing for the placement of each shell within the time interval corresponding to each particular phase (Figure 4).

Sample Collection

Our samples of archaeological limpet shells were acquired from the Quoygrew site collections housed at the Orkney Museum, in Kirkwall, Orkney. We targeted shells from phases 1 (9^{th}–10^{th} centuries) and 2 (11^{th}-13^{th} centuries), which cover a time interval spanning the Medieval Warm Period. Our initial samples included 134 limpets, 66 of which were from the Medieval Warm Period. Of these, I selected seven shells, three from phase 1 and four from phase 2 were subject to analysis. The modern limpet shells used in this study were collected by volunteers. The modern samples were recovered from Rackwick Bay, near the Quoygrew archaeological site.

Preparation of Shells

Shells were set in a metal-based epoxy resin to protect the shell during preparation, and then cut parallel to the axis of maximum growth utilizing a Buehler isomet low speed saw. The shells were subsequently cut into ~2mm thick cross section and polished to 1 µm diamond suspension grit (Buehler). Polished cross sections were then mounted to microscope slides. An Olympus DP71 12 MP digital camera mounted to an Olympus SZX7 microscope was used to analyze growth increments in the shell cross sections (Figure 5). If growth increments were difficult to discern, the shell surfaces were immersed in Mutvei's solution to enhance growth lines and increments (see Schone et al. [2005] for methodology). By observing growth lines and increments it was possible to identify fortnightly and annual growth lines, which provided guidelines for

microsampling. After identifying growth lines and targeting increments for sampling, the shells were prepared for sampling. This involved a process similar to that outlined earlier, with the exception of the immersion in Mutvei's solution. Another method used to aid in the identification of growth lines was to create extremely thin sections (< 1mm); the thin samples allowed for observation using transmitted light, which in some cases made the growth lines easier to identify.

Sampling and Geochemical Analysis

Microsampling was accomplished utilizing a Merchantek micromill sampling system, consisting of a dental drill connected to a computer-controlled microscope, which was used to identify drilling paths. This allowed for high-resolution sampling (~50-200 μm spacing). The outer calcite layers of the limpet were chosen for sampling based on results obtained by Fenger et al. [2007] during their calibration of this technique.

Approximately 30-50 μg of carbonate powder were micromilled from each sample path. Paths were drilled at 50-200 μm spacing; spacing depended on length of the drill path. In areas near the apex of the shell, increased spacing was needed to obtain enough powder to offset the shorter drill path. Appendix A shows the number of samples taken from each shell. Archaeological limpets, which range in age from three to twelve years, were sampled along their entire length. One modern limpet was also sampled, with sampling done along approximately one year's worth of growth.

Once micromilled, carbonate powder was sent to the Environmental Isotope Laboratory at the University of Arizona for isotopic analysis. Oxygen ($\delta^{18}O$) and carbon ($\delta^{13}C$) isotope ratios were measured using an automated carbonate preparation device (Kiel-III) coupled to a gas-ratio mass spectrometer (Finnigan MAT 252). Powdered samples were reacted with dehydrated phosphoric acid under vacuum at 70°C for one hour. The isotope ratio measurement was calibrated based on repeated measurements of NBS-19 (National Bureau of Standards) and NBS-18. The precision of the measurements was ±0.1‰ for $\delta^{18}O$ (1σ) and ±0.06‰ for $\delta^{13}C$ (1σ). Results are reported in per mil (‰) relative to the Vienna Pee Dee Belemnite (VPDB) standard.

Temperature Estimation

Estimated temperature was calculated using the data collected from the archaeological specimens. The equilibrium fractionation equation for calcite and water [Friedman and O'Neil, 1977, modified after Tarutani et al., 1969] was used to calculate temperature from $\delta^{18}O_{shell}$ values,

$$1000 \ln \alpha = 2.78 \times 10^6 / T^2 - 2.89$$

where *T* represents temperature and α is the fractionation factor between calcite and water. The relationship between α and δ is:

$$\alpha = (\delta_{calcite} + 1000) / (\delta_{water} + 1000)$$

where the value δ is expressed relative to VSMOW (Vienna Standard Mean Ocean Water). Because the measured calcite $\delta^{18}O$ values were reported relative to VPDB, theymust be converted to VSMOW using the equation described by Gonfiantini et al. [1995]:

$$\delta^{18}O_{(VPDB)} = (\delta^{18}O_{(VSMOW)} - 30.91) / 1.03091$$

We used a value of 0.31‰ ± 0.1‰ for the $\delta^{18}O$ of the water at the study site. This value was obtained from water samples taken from Orkney. An error of 0.1‰ corresponds to 0.5°C temperature error. Total error for each measurement was calculated by also accounting for analytical error for each sample (Appendix A). Fenger et al. [2007] observed an offset of 1.01‰ in $\delta^{18}O_{shell}$, which was consistent with offsets seen in similar study. This correction was applied to our $\delta^{18}O_{shell}$ values.

Results

Sclerochronologic analysis of seven shells revealed the limpets sampled ranged in age from 2-12 years, providing a total of 29 years of high-resolution temperature data. Each shell has variation in isotope ratios that follows a sinusoidal trend. Table 1 shows the minimum, maximum, and mean $\delta^{18}O$ and $\delta^{13}C$ values measured from the shells. Oxygen and carbon isotope ratios were plotted against distance from the apex of the shell, which represents time (Figures 6 and 7). $\delta^{13}C$ values range from -1.22‰ to 1.91‰ (QG1-7246-1), 0.18‰ to 2.07‰ (QG1-7188-1), 1.19‰ to 2.37‰ (QG1-7189-2), 0.80‰

to 2.23‰ (QG2-1061-1), -0.67‰ to1.67‰ (QG-1064-1), -0.67‰ to 1.67‰ (QG2-7180-1), and 1.55‰ to 3.01‰ (QG2-7180-2). $\delta^{18}O$ values range from 1.76‰ to 4.50‰ (QG1-7246-1), 1.53‰ to3.64‰ (QG1-7188-1), 1.03‰ to 3.67‰ (QG1-7189-2), 1.50‰ to 3.78‰ (QG2-1061-1), 1.82‰ to 3.72‰ (QG-1064-1), 1.55‰ to 3.95‰ (QG2-7180-1), and 1.64‰ to 4.18‰ (QG2-7180-2). Oxygen and carbon isotope ratios vary in a sinusoidal pattern, but are not consistently in phase. The cross-plot of $\delta^{13}C$ and $\delta^{18}O$ values for all seven archaeological shells shows no covariant trend (Figure 8).

One modern limpet was also sampled. $\delta^{13}C$ values range from -1.03‰ to 0.34‰, and average -0.19‰ ± 0.36‰. $\delta^{18}O$ values range from 0.80‰ to 3.68‰ and average 2.63‰ ± 0.73‰.

Discussion

Temperature Reconstruction

Previous studies by Fenger et al. [2007] calibrated $\delta^{18}O$ values in live-collected *P. vulgata* as a proxy for temperature. Using modern *P. vulgata* samples, they were able to reconstruct sea surface temperatures from their study site in the United Kingdom. Despite the presence of annual growth lines that formed in winter, *P. vulgata* recorded the entire seasonal range of sea surface temperature measured at the collection site. Therefore, we assume that our results represent a nearly complete range of seasonal temperature variation.

Temperature reconstruction was made using measured $\delta^{18}O$ values to estimate sea surface temperature (Table 2; Figures 9 and 10). The coldest temperatures recorded for each specimen were: 4.52°C ± 0.66°C (QG1-7246-1), 6.12°C ± 0.91°C (QG1-7188-1), 5.99°C ± 0.56°C (QG1-7189-2), 5.58°C ± 0.63°C (QG2-1061-1), 5.80°C ± 0.85°C (QG-1064-1), 4.92°C ± 0.71°C (QG2-7180-1), and 4.01°C ± 0.89°C (QG2-7180-2). Warmest temperatures recorded were: 13.75°C ± 0.64°C (QG1-7246-1), 14.73°C ± 0.52°C (QG1-7188-1), 16.91°C ± 0.95°C (QG1-7189-2), 14.86°C ± 0.96°C (QG2-1061-1), 13.50°C ± 0.63°C (QG-1064-1), 14.67°C ± 0.52°C (QG2-7180-1), and 14.29°C ± 0.96°C (QG2-7180-2). Mean summer temperatures (Table 2) were calculated by averaging the highest temperature of each year, as well as the temperatures immediately preceding and following it. This enabled us to record temperatures representative of each summer, while smoothing the records to remove extreme temperature events. The overall mean summer temperature recorded during the Medieval Warm Period was 13.4°C ± 0.7°C, while the mean winter temperature during the interval of study was 5.9°C ± 0.8°C.

Seasonal Variation

Our results show $\delta^{18}O$ and $\delta^{13}C$ values varying in a sinusoidal pattern, which we interpret to reflect seasonal variation. Isotope data can reflect growth rate, and this is important to note in the analysis of the data. Previous studies have indicated that *P. vulgata* slow their growth during the winter. In this study, dark growth increments, which denote yearly growth lines, coincide with the most positive $\delta^{18}O$ values (Figures 6 and 7), confirming the observation that this limpet slowed its growth during the winter.

However, during analysis we identified four dark growth increments on QG2-7180-2 that we attributed to yearly growth increments that do not correspond to more positive $\delta^{18}O$ values. We instead attribute these to lines formed by biological or physical disturbances. Decreased growth rates during the winter, and corresponding increased growth rates during the summer, manifest themselves in the number of data points associated with winter and summer months. Due to slower growth rates during the winter, there are a fewer number of data points recorded by the limpet. Accordingly, there are more summer data points than winter (Figures 9 and 10). The fewer number of data points recorded during winters results in the potential for the full extent of winter temperatures to not be recorded. Due to this, we excluded from analysis any temperatures from truncated records. However, based on results from Fenger et al. [2007], we assume that our results represent a nearly complete range of temperatures.

$\delta^{13}C$ values for each shell were also measured, but were difficult to interpret due to our lack of knowledge of the many variables that can affect the $\delta^{13}C$ values of marine organisms (e.g. primary productivity, pH, DIC, etc.; Fenger et al., 2007). However, it can be established that $\delta^{13}C$ values vary similarly with $\delta^{18}O$, implying that there is a seasonal influence on $\delta^{13}C$ variability. Without more detailed information on local DIC, pH, and other factors, it is difficult to draw any further conclusions.

Analysis of Paleotemperatures

Seasonal records of temperature obtained from our samples allowed us to observe

temperature and seasonality in the Orkney Islands during the Medieval Warm Period. By comparing them to modern NOAA sea surface temperature data (1961-1990) we were able to place Medieval Warm Period temperatures in context with those seen today (Figures 9 and 10). The majority of the climate record for this period consists of annual temperature records, or reconstructions biased toward summer temperatures, so the creation of a temperature archive showing seasonality during the Medieval Warm Period is an extremely valuable step in understanding paleoclimate.

The results obtained from the seven archaeological shells we sampled (Figures 9 and 10) show approximately 29 years of temperature data. Summer temperatures during the Medieval Warm Period average $13.4^{o}C \pm 0.7^{o}C$. Modern summer temperatures recorded by NOAA (1961-1990) average $12.40^{o}C \pm 0.39^{o}C$. We therefore can conclude summer temperatures during the Medieval Warm Period were slightly higher than temperatures recorded during time period 1961-1990. Winter temperatures during the Medieval Warm Period average $5.9^{o}C \pm 0.8^{o}C$. When compared to modern winter temperatures ($7.76^{o}C \pm 0.44^{o}C$), it is evident that Medieval Warm Period winters were cooler than those observed at present. Seasonality was determined by calculating the difference between average summer and winter temperatures (Table 2). During the Medieval Warm Period, seasonality averaged $7.5^{o}C$. This is greater than modern seasonality ($4.74^{o}C$) observed in the NOAA data.

When analyzing paleotemperatures, we compared them with the climatological mean from 1961-1990 to be consistent with previous studies [Mann and Jones, 2003;

Jansen et al. 2007]. However, if using NOAA SST reconstructions covering present day (1991-2009; Figure 2), we observe a slightly different relationship, which is representative of the recent global warming. Summer temperatures during this time period average 13.26°C ± 0.46°C and winter temperatures average 7.50°C ± 0.77°C. When we compare these temperatures with Medieval Warm Period temperatures obtained from our samples, we observe that summer temperatures during the Medieval Warm Period are very similar to those seen today. Winter temperatures during the Medieval Warm Period are colder than those today. Seasonality during the period 1991-2009 is 5.76°C (Medieval Warm Period seasonality is 7.5°C).

Because this is the first temperature archive from the Medieval Warm Period that allows us to observe seasonal temperature variability, it is difficult to compare our results with other temperatures recorded during the Medieval Warm Period. However, it is possible to use a comparison with modern temperatures and seasonality to draw conclusions about differences in climate between the Medieval Warm Period and today. As stated previously, we see enhanced seasonality during the Medieval Warm Period as compared to present day. This is consistent with studies of seasonality changes due to anthropogenic warming. Seasonality increases poleward, as the climate becomes less tropical [Legates and Willmott, 1990]. Consequently, as sea surface temperatures rise, we can expect to see a decrease in seasonality similar to that seen in tropical climates. If this is indeed the case, the increased seasonality observed during the Medieval Warm Period can provide interesting insight into the changing seasonality as temperatures increase.

Medieval Warm Period Climate

There is uncertainty as to the cause of the elevated temperatures characteristic of the Medieval Warm Period in northern Europe. The summer temperatures we observed during the Medieval Warm Period were similar to those observed during the present day, which are consistent with the idea of warm temperatures during the Medieval Warm Period. A persistent positive phase of the NAO has been proposed as a possible cause for the Medieval Warm Period [Lamb, 1965]. This has been further corroborated by a new NAO reconstruction by Trouet et al. [2009]. Using a tree-ring-based drought reconstruction for Morocco and a speleothem-based precipitation proxy for Scotland, they were able to reconstruct the NAO index back to 1049 AD and identify a persistent positive NAO during the Medieval Warm Period. Because a NAO+ phase has also been associated with an intensified, further-north Gulf Stream [de Coetlogon et al., 2006], the persistent NAO+, along with changes in the Gulf Stream, may have contributed to warmer temperatures seen in northern Europe during the Medieval Warm Period.

A persistent NAO+ would result in warmer winters [Trouet et al., 2009], which are seen in many of the historical datasets pertaining to the MWP [Hughes and Diaz, 1994; Grove and Switsur, 1994; Pfister et al., 1998]. One potential avenue for future study is to acquire temperature data for periods preceding and following the MWP, in order to ascertain how winter temperatures during the MWP compare to winter temperatures during different NAO phases.

Suess Effect

When Medieval Warm Period samples are compared with modern limpets, we observe a negative shift in $\delta^{13}C$ values from the Medieval Warm Period to present day (Figure 11). Modern limpets analyzed for our study have an average $\delta^{13}C$ of -0.12‰ ± 0.30‰, and range from -0.84‰ to 0.34‰. These values are consistent with data obtained by Fenger et al. [2007], where they observe average $\delta^{13}C$ values of 0.35‰ ± 0.57‰ and range from -1.54‰ to 1.43‰. $\delta^{13}C$ values obtained from Medieval Warm Period limpets averaged 1.31‰ ± 0.76‰ and range from -0.67‰ to 3.01‰ (excluding QG1-7246-1). Sample QG1-7246-1 is excluded because it has a slower growth rate than the other sampled limpets, which results in a truncated record. Fenger et al. [2007] observed this same effect while analyzing one of their longer-lived specimens.

If we assume the metabolic effects of *P. vulgata* have not changed since the Medieval Warm Period, the negative shift observed between Medieval Warm Period limpets and modern samples can be attributed to a negative shift in $\delta^{13}C_{DIC}$. This was most likely caused by the Suess effect. The Suess effect refers to the depletion of $\delta^{13}C$ in ocean and atmospheric reservoirs due to the uptake of light carbon from the burning of fossil fuels [Bacastow et al., 1996]. The Suess effect has been observed in many marine organisms, including corals, oysters and other carbonate shelled species [Nozaki et al., 1978; Surge et al., 2003; Butler et al., 2009], and so is a reasonable explanation for the negative shift observed from the Medieval Warm Period to today.

Conclusions

The Medieval Warm Period is a climate interval characterized by its inherent spatial and temporal variability. Obtaining high-resolution environmental reconstructions is consequently extremely important in reconstructing seasonal temperature variability during the Medieval Warm Period. Using the limpet *P. vulgata*, we were able to derive seasonal temperature records from the Orkney Islands during an interval of time within the Medieval Warm Period. Our reconstruction is one of the first datasets to show seasonal temperature variability that is not an annual record or biased toward summer temperatures.

Our results show that summer temperatures during the Medieval Warm Period were warmer than those seen today (1961-1990), while winter temperatures were consistently cooler during the Medieval Warm Period. This resulted in enhanced seasonality during the Medieval Warm Period when compared to today. We were also able to detect a shift in carbon isotope ratios that we attribute to the Suess effect.

With further work, we hope to be able to extend our temperature reconstruction, and compare Medieval Warm Period temperatures to climate preceding and following this interval, so that we may obtain a better understanding of past climate. This will enable us to evaluate not only the potential causes of this climate interval, but also the effects climate change had on the inhabitants of our study site in the Orkneys.

Acknowledgements

Thanks to Dr. Donna Surge, Dr .Jonathan Lees, and Dr. Laurie Steponaitis for their comments, advice, and discussion; they greatly contributed to the quality of this thesis. Thanks also to Joel Hudley, Dr. Jose Rafa Garcia-March, and Ting Wang for their help and advice. I would like to thank Dr. Drew Coleman for letting me use his lab equipment, and Dr. David Dettman and the University of Arizona Environmental Isotope Laboratory for running my analyses. Anne Brundle and the Orkney Museum provided the samples used in this study. Funding for this project was provided by the National Geographic Society.

References

Alley, R.B., 2000. *The Two Mile Time Machine*, Princeton University Press, Princeton, NJ, 229p.

Bacastow, R.B., Keeling, C.D., Lueker, T.J., Wahlen, M., 1996. The ^{13}C Suess effect in the world surface oceans and its implications for oceanic uptake of CO_2: analysis of observations at Bermuda. *Global Biogeochemical Cycles*, 10, 335-345.

Barrett, J.H., Richards, M.P., 2004. Identity, gender, religion and economy: New isotope and radiocarbon evidence for marine resource intensification in early historic Orkney, Scotland, UK. *European Journal of Archaeology,* 7, 249-271.

Bourget, E., 1980. Barnacle shell growth and its relationship to environmental factors, in *Skeletal Growth of Aquatic Organisms: Biological Records of Environmental Change*, edited by D.C. Rhoads and R.A. Lutz, Plenum Press, New York, 469-491.

Branch, G.M., 1981. The biology of limpets: Physical factors, energy flow, and ecological interactions. *Oceanography and Marine Biology an Annual Review*, 19, 235-280.

Brazdil, R., Pfister, C., Wanner, H., von Storch, H., Luterbacher, J., 2005. Historical climatology in Europe – The State of the Art. *Climate Change,* 70, 363-430.

Butler, P.G., Scourse, J.D., Richardson, C.A., Wanamaker Jr., A.D., Bryant, C.L., Bennell, J.D., 2009. Continuous marine radiocarbon reservoir calibration and the ^{13}C Suess effect in the Irish Sea: results from the first multi-centennial shell-based marine master chronology. *Earth and Planetary Science Letters*, 279, 230-241.

de Coetlogon, G., Frankignoul, C., Bentsen, M., Delon, C., Haak, H., Masina, S., Pardaens, A., 2006. Gulf Stream variability in five oceanic general circulation models. *Journal of Physical Oceanography,* 36, 2119-2135.

Cohen, J.E., Christopher, S., Mellinger, A., Gallup, J., Sachs, J., Vitousek, P.M., Mooney, H.A., 1997. Estimates of coastal populations. *Science*, 278, 1209-1213.

Cook, E.R., D'Arrigo, R.D., Mann, M.E., 2002. A Well-Verified, Multiproxy Reconstruction of the Winter North Atlantic Oscillation Index since A.D. 1400. *Journal of Climate*, 15, 1754-1764.

Crisp, D.J., 1965. Observations on the effect of climate and weather on marine communities, in *The Biological Significance of Climatic Changes in Britain*, edited by C.G. Johnson and L.P. Smith, Elsevier, New York, 73-77.

Crowley, T.J., Lowery, T.S., 2000. How warm was the medieval warm period? *Ambio*, 29, 51-54.

D'Arrigo, R., Wilson, R., Jacoby, G., 2006. On the long-term context for late twentieth century warming. *Journal of Geophysical Research*, 111.

Dansgaard, W., Johnsen, S.J., Clausen, H.B., Dahl-Jensen, D., Gundestrup, N., Hammer, C.U., 1984. North Atlantic climatic oscillations revealed by deep Greenland ice cores, *Geophysical Monograph Series*, 29, 288-298.

Ekaratne, S.U.K., Krisp, D.J., 1982. Tidal micro-growth bands in intertidal gastropod shells, with an evaluation of band-dating techniques, *Proceedings of the Royal Society of London, Series B*, 214, 305-323.

Ekaratne, S.U.K., Krisp, D.J., 1984. Seasonal growth studies of intertidal gastropods from shell micro-growth band measurements, including a comparison with alternative methods, *Journal of Marine Biological Association of the UK*, 64, 13-210.

Epstein, S., Buchsbaum, R., Lowenstam, H., Urey, H.C., 1951. Carbonate-water isotopic temperature scale. *Geological Society of America Bulletin*, 62, 417-425.

Esper, J., Cook, E.R., Schweingruber, F.H., 2002. Low-frequency signals in long tree-ring chronologies for reconstructing past temperature variability. *Science,* 295, 2250-2253.

Fenger, T., Surge, D., Schone, B., Milner, N., 2007. Sclerochronology and geochemical variation in limpet shells (*Patella vulgata*): A new archive to reconstruct coastal sea surface temperature. *Geochemistry, Geophysics, Geosystems*, 8.

Friedman, I., O'Neil, J.R., 1977. Compilation of stable isotope fractionation factors of geochemical interest, in *Data of Geochemistry*, edited by M. Fleischer, U.S. Government Printing Office, Washington, DC, 1-12.

Gonfiantini, R., Stichler, W., Rozanski, K., 1995. Standards and intercomparison materials distributed by the International Atomic Energy Agency for stable isotope measurements, in *References and Intercomparison Materials for Stable isotopes of Light Elements*, edited by the Isotope Hydrology Section of the International Atomic Energy Agency, IAEA, Vienna, Austria, 13-29.

Goosse, H., Arzel, O., Luterbacher, J., Mann, M.E., Renssen, H., Riedwyl, N., Timmermann, A., Xoplake, E., Wanner, H., 2006. The origin of the European "Medieval Warm Period." *Climate of the Past,* 2: 99-113.

Grove, J.M., Switsur, R., 1994. Glacial geological evidence for the Medieval Warm Period. *Climate Change,* 26, 143-169.

Hughes, M.K., Diaz, H.F., 1994. Was there a "Medieval Warm Period," and if so, where and when? *Climate Change*, 26, 109-142.

Hunt, B.G., 2006. The Medieval Warm Period, the Little Ice Age and simulated climatic variability. *Climate Dynamics*, 27: 677-694.

Hurrell, J.W., Van Loon, H., 1997. Decadal variations in climate associated with the North Atlantic Oscillation. *Climatic Change,* 36, 301-326.

Jansen, E., J. Overpeck, K.R. Briffa, J.-C. Duplessy, F. Joos, V. Masson-Delmotte, D. Olago, B. Otto-Bliesner, W.R. Peltier, S. Rahmstorf, R. Ramesh, D. Raynaud, D. Rind, O. Solomina, R. Villalba and D. Zhang, 2007: Palaeoclimate. In: Climate Change 2007: The Physical Science Basis. Contribution of Working Group I to the Fourth Assessment Report of the Intergovernmental Panel on Climate Change [Solomon, S., D. Qin, M. Manning, Z. Chen, M. Marquis, K.B. Averyt, M. Tignor and H.L. Miller (eds.)]. Cambridge University Press, Cambridge, United Kingdom and New York, NY, USA.

Jenkins, S.R., Hartnoll, R.G., 2001. Food supply, grazing activity, and growth rate in the limpet *Patella vulgata* L.: A comparison between exposed and sheltered shores, *Journal of Experimental Marine Biology and Ecology*, 258, 123-139.

Jennings, E., Allot, N., 2006. Position of the Gulf Stream influences lake nitrate concentrations in SW Ireland. *Aquatic Sciences*, 68, 482-489.

Jones, D.S., 1983. Sclerochronology: Reading the record of the molluscan shell. *American Scientist*, 71, 384-391.

Jones, D.S., Quitmyer, I.R., 1996. Marking time with bivalve shells: Oxygen isotopes and season of annual increment formation, *Palaios,* 11, 340-346.

Jones, P.D., Mann, M.E., 2004. Climate over past millennia. *Reviews of Geophysics*, 42, 1-42.

Lamb, H.H., 1965. The early Medieval warm epoch and its sequel. *Palaeogeography, Palaeoclimatology, Palaeoecology*, 1: 13-37.

Legates, D.R., Willmott, C.J., 1990. Mean seasonal and spatial variability in global surface air temperature. *Theoretical and Applied Climatology*, 41, 11-21.

Lewis, J.R., Bowman, R.S., 1975. Local habitat-induced variations in the population dynamics of *Patella vulgata* L., *Journal of Experimental Marine Biology and Ecology*, 17, 165-203.

Lund, D.C., Lynch-Stieglitz, J., Curry, W.B., 2006. Gulf Stream density structure and transport during the past millennium. *Nature*, 444, 601-604.

Mann, M.E., 2002. The Earth system: physical and chemical dimensions of global environmental change, Volume 1, in *Encyclopedia of Global Environmental Change,* edited by MacCracken, M.C. and Perry, J.S., 2002.

Mann, M.E., 2007. Climate Over the Past Two Millennia. *Annual Review of Earth and Planetary Sciences*, 35, 111-136.

Mann, M.E., Jones, P.D., 2003. Global surface temperatures over the past two millennia. *Geophysical Research Letters*, 15, 1-4.

Milner, N., Barrett, J., Welsh, J., 2007. Marine resource intensification in Viking Age Europe: the molluscan evidence from Quoygrew, Orkney. *Journal of Archaeological Science*, 34, 1461-1472.

Minobe, S., Kuwano-Yoshida, A., Komori, N., Xie, S., Small, R.J., 2008. Influence of the Gulf Stream on the troposphere. *Nature*, 452, 206-209.

NOAA_ERSST_V3 data provided by the NOAA/OAR/ESRL PSD, Boulder, Colorado, USA, from their Web site at http://www.cdc.noaa.gov/

Nozaki, Y., Rye, D.M., Turekian, K.K., Dodge, R.E., 1978. A 200 year record of carbon-13 and carbon-14 variations in a Bermuda coral. *Geophysical Research Letters,* 5, 825-828.

Ogilvie, A.E.J., 1991. Climatic changes in Iceland, AD 865 to 1598. *Acta. Archeol.,* 61, 233-251.

Pfister, C., Luterbacher, J., Schwarz-Zanetti, G., Wegmann, M., 1998. Winter air temperature variations in western Europe during the Early and High Middle Ages (AD 750-1300). *The Holocene,* 8: 535-552.

Schifano, G., Censi, P., 1986. Oxygen and carbon isotope composition, magnesium and strontium contents of calcite from a subtidal *Patella coerulea* shell, *Chem. Geol.*, 58, 325-331.

Schone, B.R., Dunca, E., Fiebig, J., Pfeiffer, M., 2005. Mutvei's solution: An ideal agent for resolving microgrowth structures of biogenic carbonates. *Palaeogeography, Palaeoclimatology, Palaeoecology*, 228, 149-166.

Shackleton, N.J., 1973. Oxygen isotope analysis as a means of determining season of occupation of prehistoric midden sites. *Archaeometry,* 15, 133-141.

Small, C., 2004. Continental Physiography, Climate, and the Global Distribution of Human Population. *Current Anthropology*, 45, 269-277.

Stenseth, N.C., Ottersen, G., Hurrell, J.W., Mysterud, A., Lime, M., Chan, K., Yoccoz, N.G., Adlandsvik, B., 2003. Studying climate effects on ecology through the use of climate indices: the North Atlantic Oscillation, El Nino Southern Oscillation and beyond. *Proceedings of the Royal Society of London*, 270, 2087-2096.

Stott, K.J., Austin, W.E.N., Sayer, M.D.J., Weidman, C.R., Cage, A.G., Wilson, R.J.S., 2009. The potential of *Arctica islandica* growth records to reconstruct coastal climate in north west Scotland, UK. *Quaternary Science Reviews,* in press.

Surge, D.M., Lohmann, K.C., Goodfriend, G.A., 2003. Reconstructing estuarine conditions: oyster shells as recorders of environmental change, Southwest Florida. *Estuarine, Coastal and Shelf Science*, 57, 737-756.

Surge, D.M., Walker, K.J., 2005. Oxygen isotope composition of modern and archaeological otoliths from the estuarine hardhead catfish (*Ariopsis felis*) and their potential to record low-latitude climate change. *Palaeogeography, Palaeoclimatology, Palaeoecology*, 228, 179-191.

Surge, D.M., Walker, K.J., 2006. Geochemical variation in microstructural shell layers of the southern quahog (*Mercenaria campechiensis*): Implications for reconstructing seasonality. *Palaeogeography, Palaeoclimatology, Palaeoecology*, 237, 182-190.

Taylor, A.H., 1995. North-south shifts of the Gulf Stream and climatic connection with the abundance of zooplankton in the UK and its surrounding seas. *ICES Journal of Marine Science*, 52, 711-721.

Tarutani, T., Clayton, R.N., Mayeda, T.K., 1969. The effect of polymorphism and magnesium substitution on oxygen isotope fractionation between calcium carbonate and water. *Geochimica et Cosmochimica Acta*, 33, 987-996

Taylor, A.H., Stephens, J.A., 1998. The North Atlantic Oscillation and the latitude of the Gulf Stream. *Tellus,* 50A, 134-142.

Trouet, V., Esper, J., Graham, N.E., Baker, A., Scourse, J.D., Frank, D.C., 2009. Persistent positive North Atlantic Oscillation mode dominated the Medieval Climate Anomaly. *Science*, 324, 78-80.

Walker, K.J., Surge, D., 2006. Developing oxygen isotope proxies from archaeological sources for the study of Late Holocene human-climate interactions in coastal southwest Florida. *Quaternary International,* 150, 3-11.

Wanner, H., Bronnimann, S., Casty, C., Gyalistras, D., Luterbacher, J., Schmutz, C., Stephenson, D.B., Xoplaki, E., 2001. North Atlantic Oscillation – Concepts and Studies. *Surveys in Geophysics*, 22, 321-382.

Williams, D.F., Arthur, M.A., Jones, D.S., Healy-Williams, N., 1982. Seasonality and mean annual sea surface temperatures from isotopic and sclerochronological records. *Nature,* 296, 432-434.

Table 1: Carbon and oxygen isotope ratios.

	δ^{13}C‰ (VPDB)			δ^{18}O‰ (VPDB)		
Sample No.	**Min.**	**Max.**	**Mean**	**Min.**	**Max.**	**Mean**
QG1-7188-1	0.180	2.067	1.238 ± 0.45	1.533	3.635	2.403 ± 0.60
QG1-7189-2	1.186	2.370	1.694 ± 0.28	1.030	3.669	2.338 ± 0.59
QG1-7246-1	-1.222	1.908	0.067 ± 0.70	1.763	4.050	2.744 ± 0.55
QG2-1061-1	0.797	2.235	1.564 ± 0.32	1.502	3.775	2.622 ± 0.62
QG2-1064-1	-0.669	1.668	0.510 ± 0.57	1.821	3.719	2.515 ± 0.52
QG2-7180-1	-0.674	1.671	0.749 ± 0.49	1.547	3.946	2.365 ± 0.58
QG2-7180-2	1.552	3.010	2.275 ± 0.35	1.635	4.182	2.576 ± 0.65

Table 2: Estimated temperatures.

	Temperature (^{o}C)				
Sample No.	**Mean summer**	**Mean winter**	**Max.**	**Min.**	**Seasonality**
QG1-7188-1	13.31 ± 0.24	5.95 ± 0.24	14.73	6.12	7.36 ± 0.34
QG1-7189-2	13.49 ± 0.09	6.79 ± 1.13	16.91	5.99	6.70 ± 1.13
QG1-7246-1	12.24 ± 0.63	6.66 ± 1.09	13.75	4.52	5.58 ± 1.26
QG2-1061-1	12.39 ± 0.10	5.71 ± 0.13	14.86	5.58	6.69 ± 0.16
QG2-1064-1	12.20 ± 0.53	6.07 ± 0.26	13.50	5.80	6.14 ± 0.59
QG2-7180-1	12.73 ± 0.64	5.79 ± 0.80	14.67	4.92	6.95 ± 1.02
QG2-7180-2	12.23 ± 0.99	4.74 ± 1.03	14.29	4.01	7.49 ± 1.43

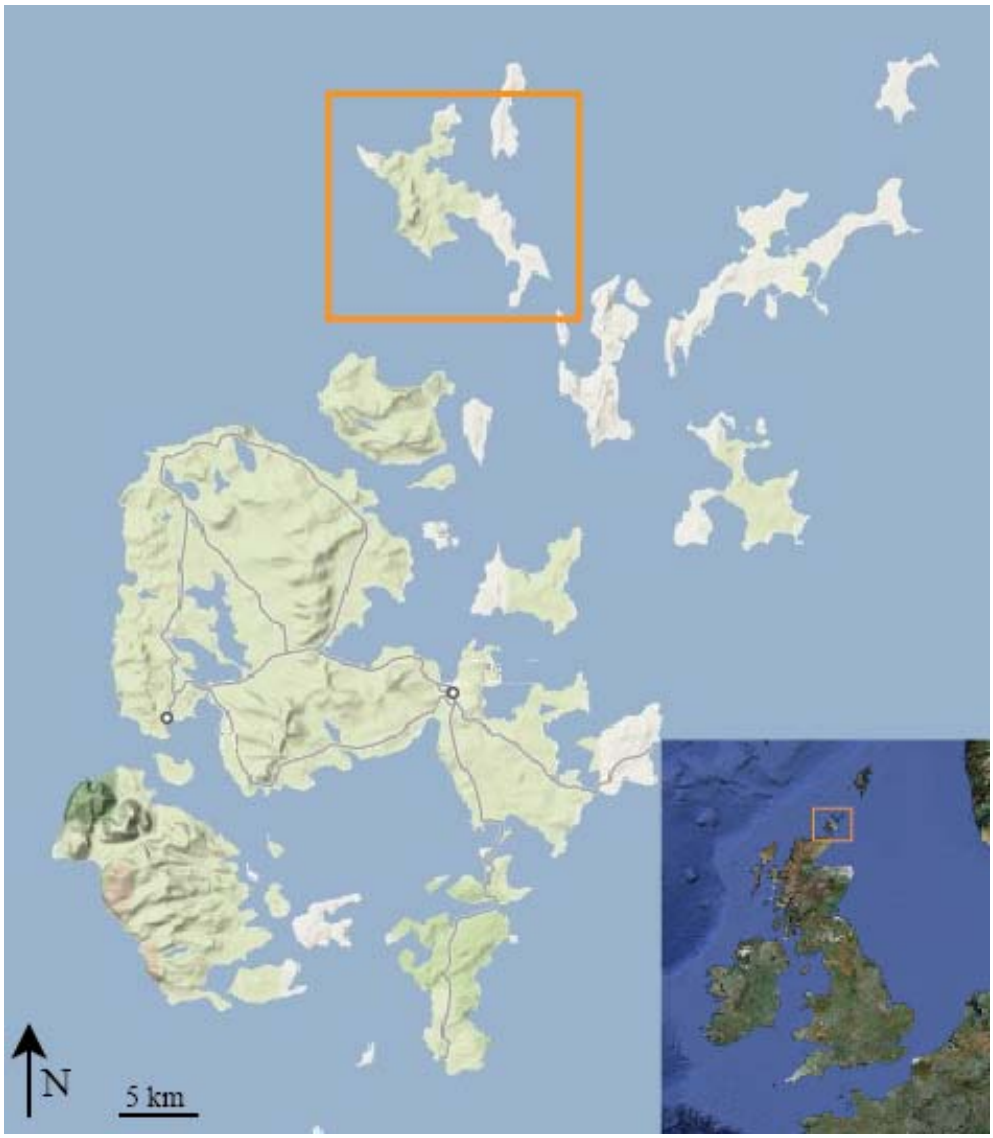

Figure 1: Map of study area in the Orkney Islands, United Kingdom. Inset at right shows the location of the Orkneys relative to the UK, and the orange box outlines our study area at the isle of Westray. Figure modified from Google Maps.

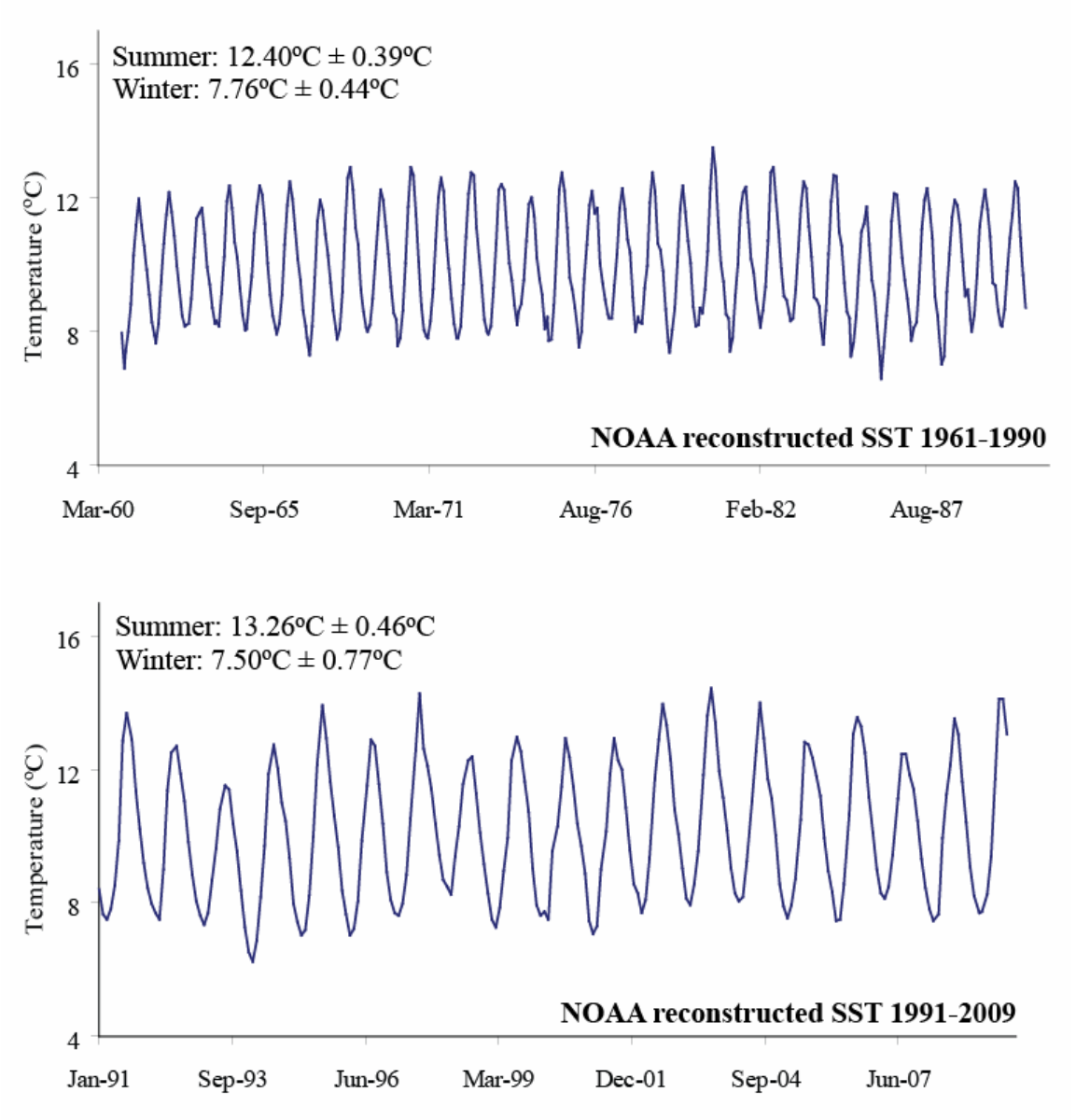

Figure 2: NOAA reconstructed sea surface temperatures from 1961-1990 (top) and from 1991-2009 (bottom) from the Orkney Islands. These temperatures were used in conjunction with estimated MWP temperatures to characterize Orkney climate during the MWP. Mean summer and winter temperatures are noted on the graph.

Figure 3: Quoygrew, Orkney. Aerial photograph of the study site on the isle of Westray, Orkney. The Viking settlement of Quoygrew is undergoing excavation; red boxes indicate midden locations from which samples were obtained (a – farm mound; b – midden; c – fish midden).

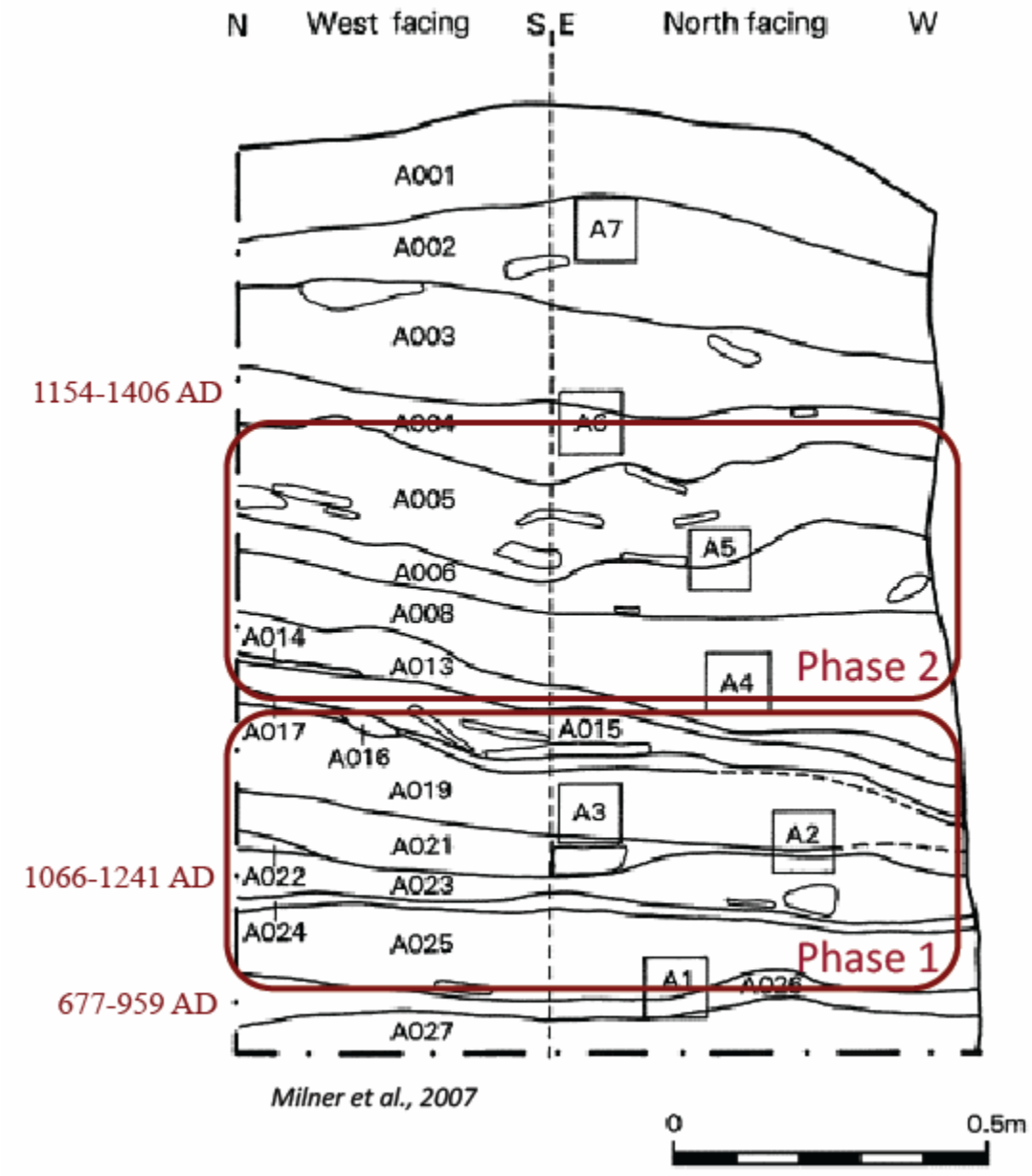

Figure 4: Quoygrew chronostratigraphy. Stratigraphy of the middens found at the Quoygrew settlement. Middens were dated using radiocarbon and artifactual evidence; radiocarbon dates are shown to the side of the figure. Our study targeted phases 1 and 2, which spanned the Medieval Warm Period. Figure modified from Milner et al. [2007].

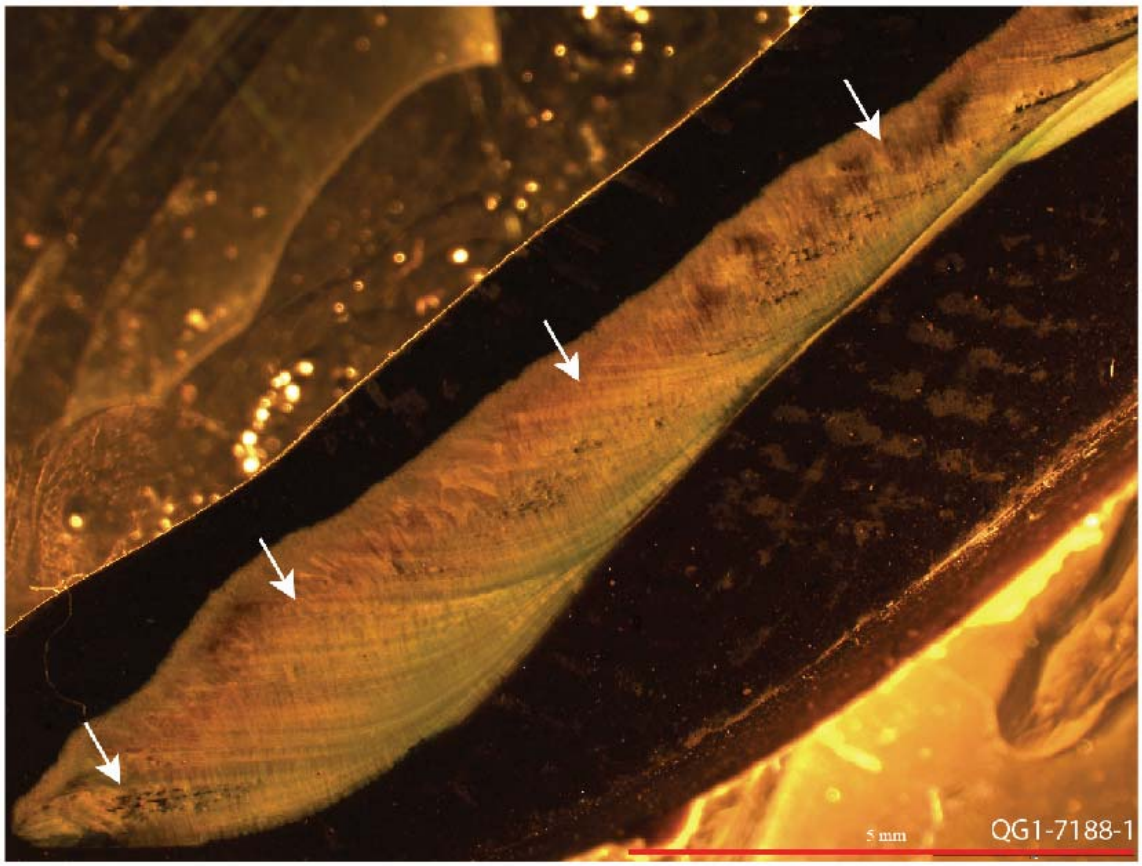

Figure 5: Limpet cross section. White arrows indicate yearly growth increments. We used annual growth lines to guide fortnightly sampling, allowing us to obtain high-resolution climate data.

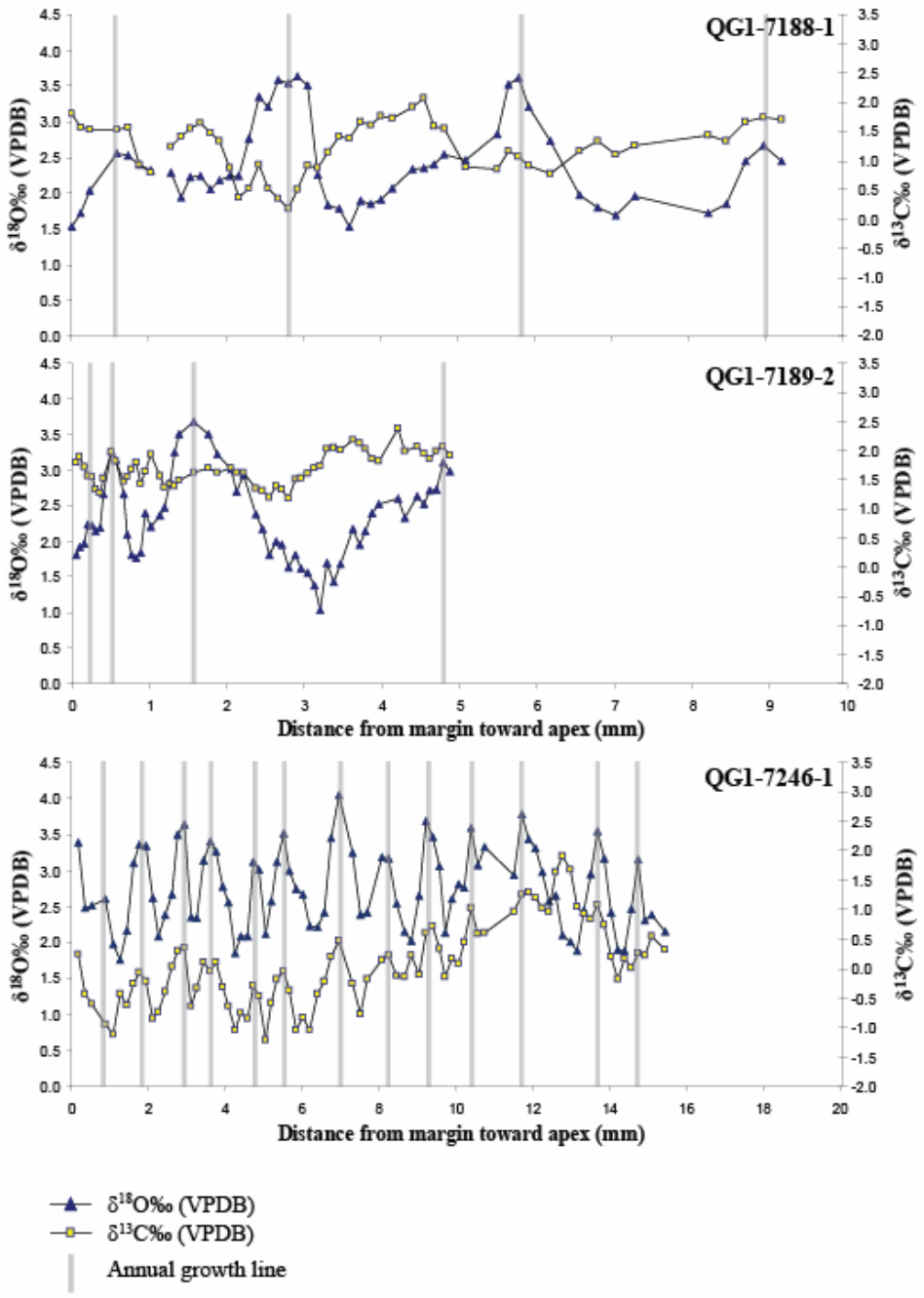

Figure 6: Phase 1 oxygen and carbon isotope ratios. Plots show $\delta^{18}O$ and $\delta^{13}C$ versus distance from the apex of the shell, which represents time.

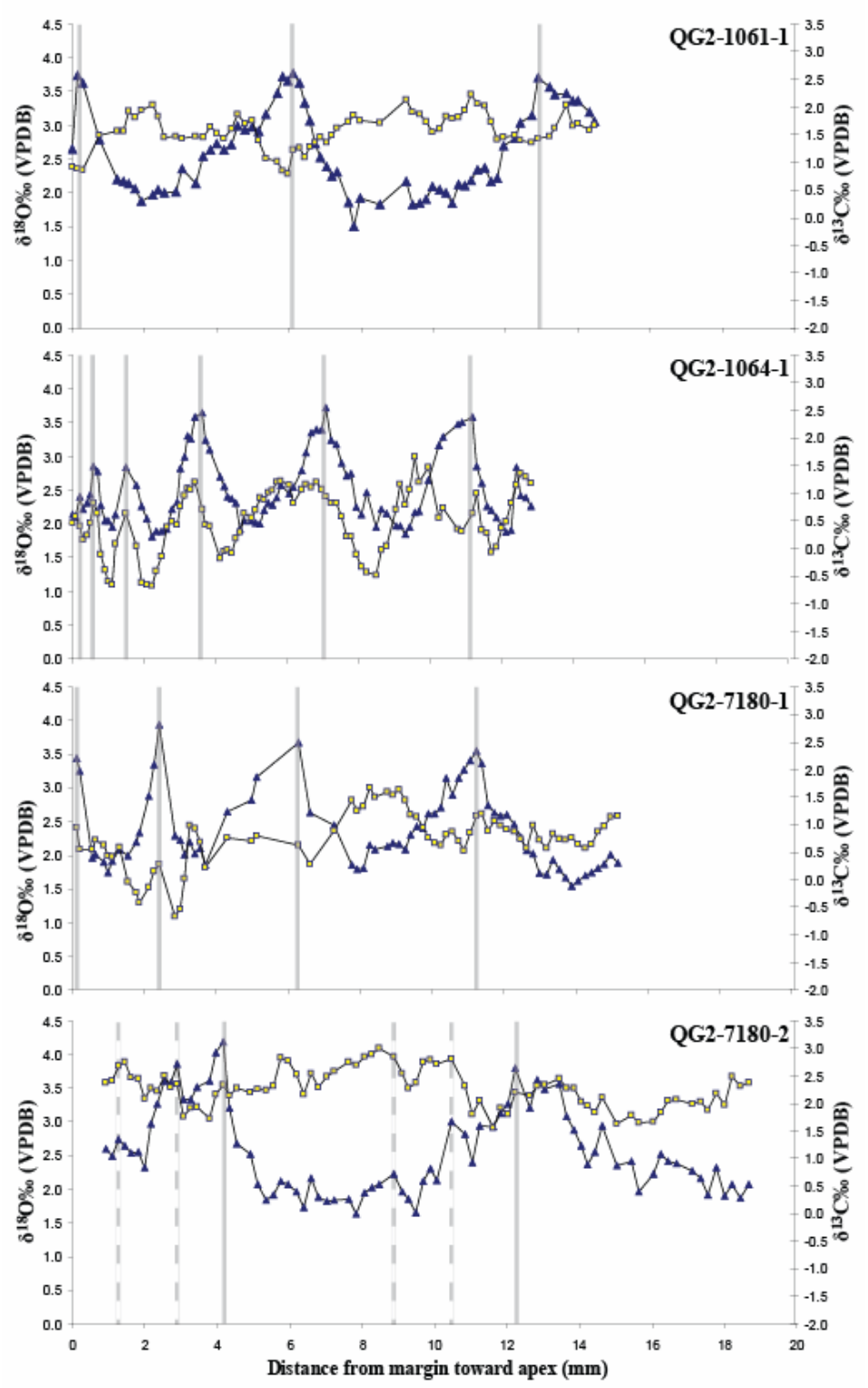

Figure 7: Phase 2 oxygen and carbon isotope ratios. Plots show $\delta^{18}O$ and $\delta^{13}C$ versus distance from the apex of the shell, which represents time. Key is the same as that of Figure 6; dashed gray bars represent disturbance lines.

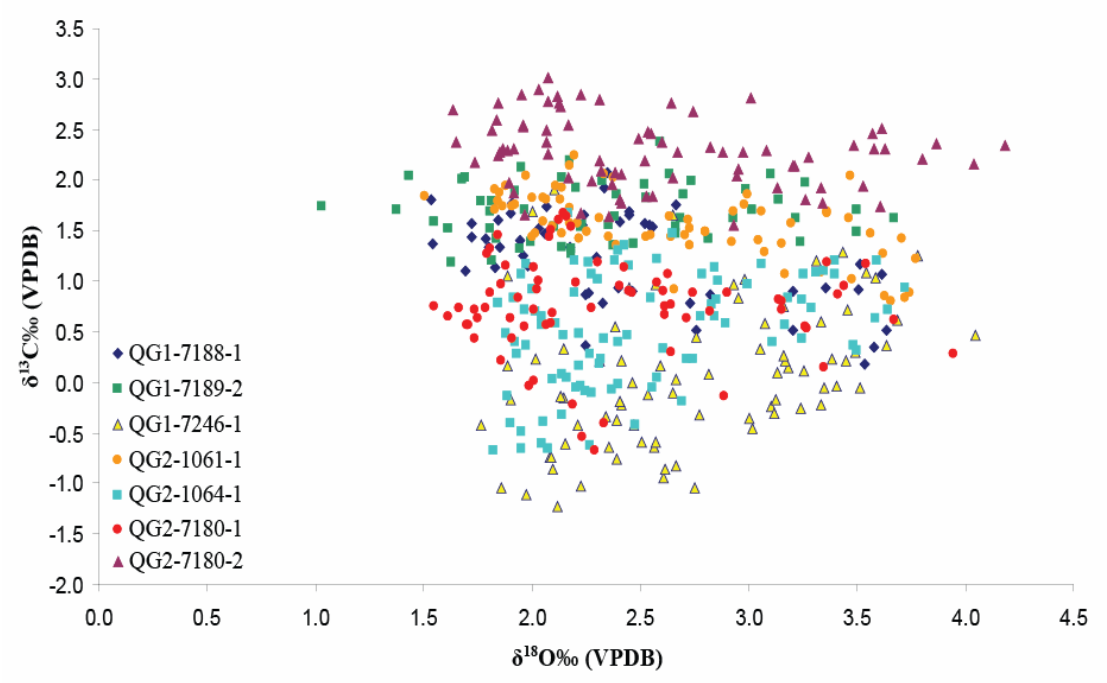

Figure 8: Crossplot of oxygen and carbon isotope ratios.

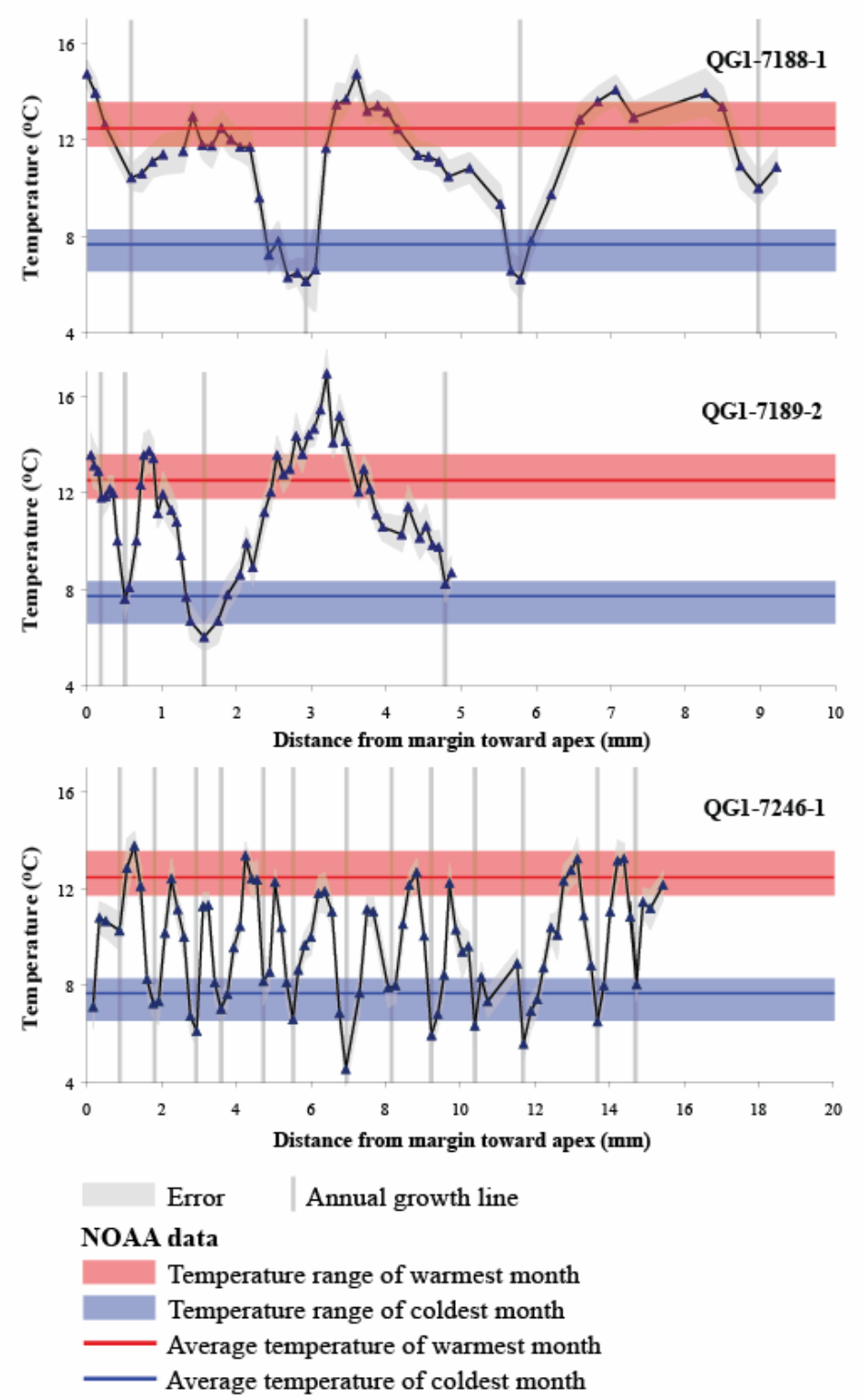

Figure 9: Estimated temperature for phase 1 shells. Plots show estimated temperature versus distance from the apex of the shell, which represents time. NOAA data represents SST reconstruction from 1961-1990.

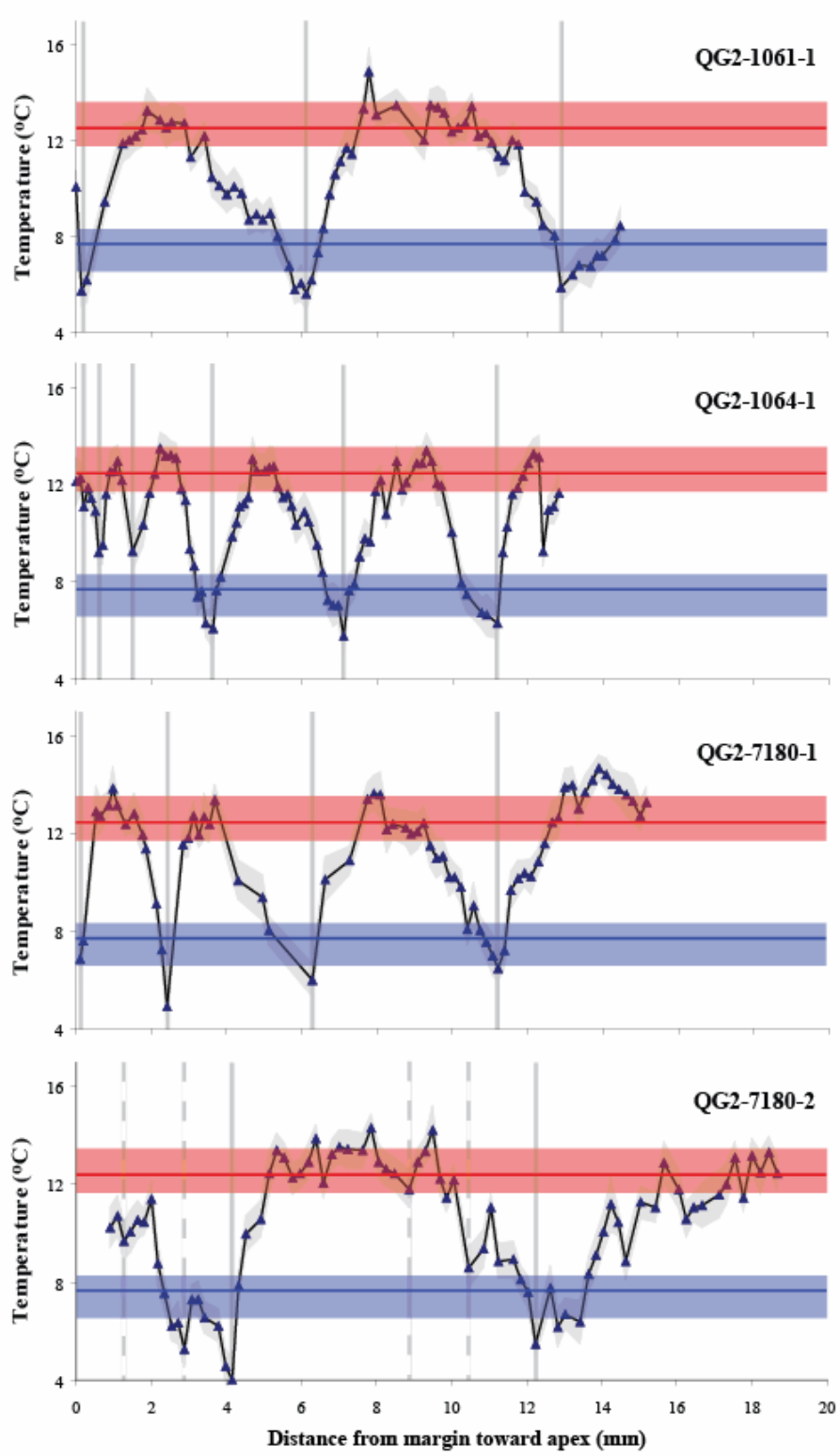

Figure 10: Estimated temperature for phase 2 shells. NOAA data represents SST reconstruction from 1961-1990. Key is the same as that of Figure 9; dashed gray bars represent disturbance lines.

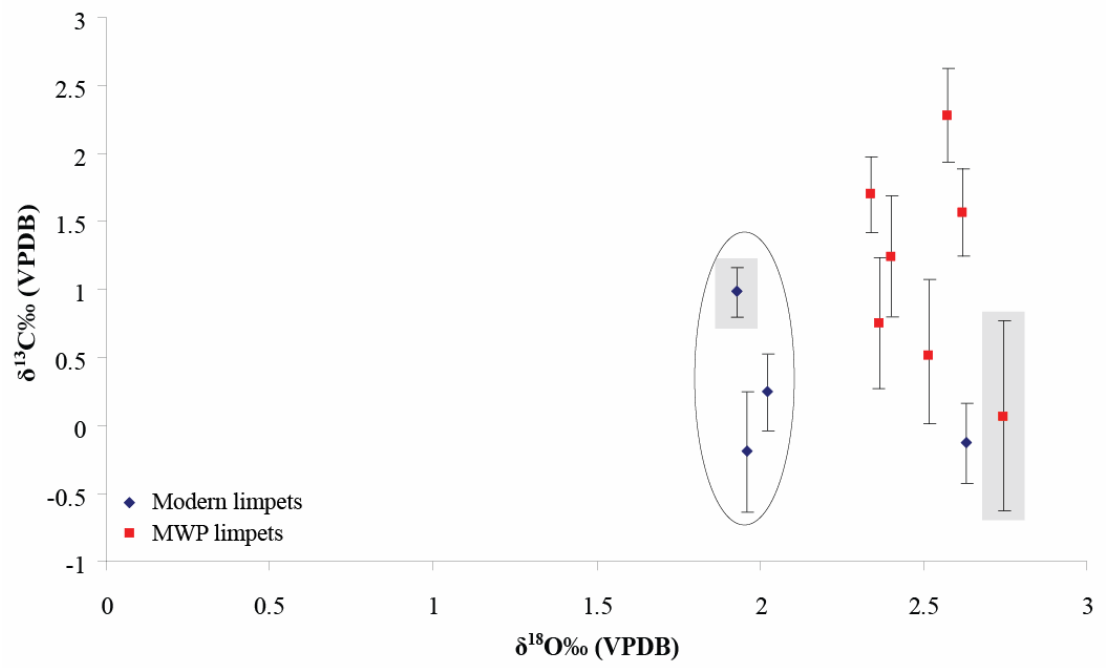

Figure 11: Mean carbon and isotope ratios for each shell. Note the negative shift in $\delta^{13}C$ values from the MWP to present. Shaded gray areas indicate longer-lived shells; slow growth rates for these specimens result in a truncated record. Circled modern data obtained from Fenger et al. [2007].

APPENDIX A: Oxygen and carbon isotope ratios

QG1-7188-1 (sampled 10/4/2008)

Sample ID	δ13C (VPDB)	δ13C ±	δ18O (VPDB)	δ18O ±	Distance (um)	T °C	comments
QG1-7188-1	1.80	0.041	1.53	0.005	0	14.7	growing edge
QG1-7188-1	1.57	0.044	1.72	0.024	118	13.9	
QG1-7188-1	1.52	0.051	2.03	0.020	236	12.6	
QG1-7188-1	1.54	0.019	2.56	0.008	590	10.4	growth line
QG1-7188-1	1.56	0.035	2.52	0.062	734	10.6	
QG1-7188-1	0.93	0.033	2.40	0.045	878	11.1	
QG1-7188-1	0.79	0.023	2.33	0.071	1022	11.4	
QG1-7188-1	0.78	0.033	2.93	0.064	1166	8.9	
QG1-7188-1	1.24	0.047	2.29	0.086	1292	11.5	
QG1-7188-1	1.41	0.011	1.94	0.002	1418	13.0	
QG1-7188-1	1.55	0.006	2.23	0.011	1544	11.8	
QG1-7188-1	1.65	0.043	2.24	0.100	1670	11.8	
QG1-7188-1	1.47	0.027	2.06	0.047	1796	12.5	
QG1-7188-1	1.34	0.029	2.18	0.051	1922	12.0	
QG1-7188-1	0.87	0.029	2.25	0.021	2048	11.7	
QG1-7188-1	0.37	0.021	2.25	0.079	2174	11.7	
QG1-7188-1	0.52	0.041	2.76	0.043	2300	9.6	
QG1-7188-1	0.94	0.051	3.35	0.070	2426	7.2	
QG1-7188-1	0.52	0.055	3.21	0.074	2552	7.8	
QG1-7188-1	0.35	0.006	3.58	0.012	2678	6.3	
QG1-7188-1	0.18	0.042	3.54	0.014	2804	6.5	
QG1-7188-1	0.51	0.032	3.64	0.106	2930	6.1	growth line
QG1-7188-1	0.91	0.105	3.51	0.327	3056	6.6	
QG1-7188-1	0.88	0.013	2.26	0.049	3193	11.7	
QG1-7188-1	1.14	0.013	1.83	0.092	3330	13.5	
QG1-7188-1	1.41	0.024	1.78	0.021	3467	13.7	
QG1-7188-1	1.37	0.006	1.54	0.066	3604	14.7	
QG1-7188-1	1.67	0.041	1.90	0.014	3741	13.2	
QG1-7188-1	1.60	0.028	1.84	0.029	3878	13.4	
QG1-7188-1	1.77	0.033	1.91	0.043	4015	13.1	
QG1-7188-1	1.73	0.028	2.07	0.072	4152	12.5	
QG1-7188-1	1.93	0.029	2.33	0.018	4426	11.4	
QG1-7188-1	2.07	0.004	2.35	0.009	4563	11.3	
QG1-7188-1	1.60	0.021	2.40	0.016	4700	11.1	
QG1-7188-1	1.56	0.054	2.54	0.028	4837	10.5	
QG1-7188-1	0.90	0.054	2.46	0.028	5111	10.8	
QG1-7188-1	0.86	0.026	2.82	0.057	5522	9.4	
QG1-7188-1	1.16	0.020	3.51	0.054	5659	6.6	
QG1-7188-1	1.06	0.024	3.61	0.083	5796	6.2	growth line
QG1-7188-1	0.90	0.005	3.20	0.044	5933	7.8	
QG1-7188-1	0.79	0.031	2.73	0.050	6207	9.7	
QG1-7188-1	1.16	0.032	1.98	0.044	6583	12.8	
QG1-7188-1	1.33	0.019	1.80	0.018	6822	13.6	
QG1-7188-1	1.11	0.008	1.69	0.023	7061	14.1	
QG1-7188-1	1.25	0.017	1.96	0.027	7300	12.9	
QG1-7188-1	1.44	0.057	1.72	0.110	8256	13.9	
QG1-7188-1	1.34	0.012	1.85	0.081	8495	13.4	
QG1-7188-1	1.66	0.010	2.45	0.093	8734	10.9	
QG1-7188-1	1.75	0.037	2.67	0.044	8973	10.0	growth line
QG1-7188-1	1.70	0.066	2.45	0.049	9212	10.9	

QG1-7189-2 (sampled 9/8/2008)

Sample ID	δ13C (VPDB)	δ13C ±	δ18O (VPDB)	δ18O ±	Distance (um)	T °C	comments
QG1-7189-2	1.79	0.027	1.81	0.090	51	13.5	
QG1-7189-2	1.89	0.060	1.92	0.100	102	13.1	
QG1-7189-2	1.71	0.018	1.97	0.082	153	12.9	
QG1-7189-2	1.56	0.014	2.23	0.071	204	11.8	growth line
QG1-7189-2	1.54	0.009	2.22	0.028	255	11.8	
QG1-7189-2	1.34	0.028	2.14	0.010	306	12.2	
QG1-7189-2	1.27	0.032	2.18	0.044	357	12.0	
QG1-7189-2	1.53	0.043	2.66	0.043	408	10.0	
QG1-7189-2	1.97	0.022	3.26	0.070	510	7.6	growth line
QG1-7189-2	1.81	0.003	3.14	0.022	561	8.1	
QG1-7189-2	1.46	0.049	2.66	0.077	663	10.0	
QG1-7189-2	1.55	0.035	2.10	0.097	714	12.3	
QG1-7189-2	1.68	0.064	1.81	0.086	765	13.6	
QG1-7189-2	1.79	0.003	1.77	0.082	827	13.7	
QG1-7189-2	1.42	0.017	1.84	0.053	889	13.4	
QG1-7189-2	1.64	0.021	2.39	0.014	951	11.1	
QG1-7189-2	1.92	0.054	2.20	0.102	1013	11.9	
QG1-7189-2	1.55	0.005	2.36	0.085	1137	11.3	
QG1-7189-2	1.37	0.046	2.47	0.060	1199	10.8	
QG1-7189-2	1.42	0.023	2.82	0.037	1261	9.4	
QG1-7189-2	1.38	0.026	3.24	0.021	1323	7.7	
QG1-7189-2	1.49	0.039	3.50	0.061	1385	6.7	
QG1-7189-2	1.63	0.007	3.67	0.015	1571	6.0	growth line
QG1-7189-2	1.70	0.007	3.50	0.101	1757	6.7	
QG1-7189-2	1.63	0.017	3.22	0.053	1881	7.8	
QG1-7189-2	1.70	0.050	3.01	0.037	2047	8.6	
QG1-7189-2	1.61	0.020	2.69	0.038	2130	9.9	
QG1-7189-2	1.63	0.026	2.93	0.067	2213	8.9	
QG1-7189-2	1.36	0.019	2.38	0.058	2379	11.2	
QG1-7189-2	1.32	0.019	2.18	0.059	2462	12.0	
QG1-7189-2	1.20	0.019	1.81	0.065	2545	13.5	
QG1-7189-2	1.39	0.014	1.99	0.060	2628	12.8	
QG1-7189-2	1.33	0.016	1.94	0.012	2711	13.0	
QG1-7189-2	1.19	0.038	1.63	0.097	2794	14.3	
QG1-7189-2	1.51	0.054	1.81	0.049	2877	13.6	
QG1-7189-2	1.52	0.031	1.62	0.010	2960	14.4	
QG1-7189-2	1.60	0.010	1.55	0.054	3043	14.7	
QG1-7189-2	1.71	0.045	1.37	0.035	3126	15.4	
QG1-7189-2	1.74	0.044	1.03	0.103	3209	16.9	
QG1-7189-2	2.03	0.010	1.69	0.024	3292	14.1	
QG1-7189-2	2.04	0.021	1.43	0.090	3375	15.2	
QG1-7189-2	2.00	0.062	1.68	0.106	3458	14.1	
QG1-7189-2	2.19	0.015	2.17	0.030	3624	12.0	
QG1-7189-2	2.13	0.015	1.95	0.017	3707	13.0	
QG1-7189-2	2.03	0.029	2.14	0.079	3790	12.2	
QG1-7189-2	1.85	0.035	2.39	0.035	3873	11.1	
QG1-7189-2	1.82	0.017	2.52	0.020	3956	10.6	
QG1-7189-2	2.37	0.029	2.60	0.056	4205	10.3	
QG1-7189-2	2.00	0.009	2.33	0.101	4288	11.4	
QG1-7189-2	2.06	0.035	2.63	0.098	4454	10.1	
QG1-7189-2	1.95	0.039	2.52	0.101	4537	10.6	
QG1-7189-2	1.85	0.010	2.70	0.017	4620	9.8	

QG1-7189-2	2.00	0.021	2.73	0.055	4703	9.7	
QG1-7189-2	2.06	0.026	3.11	0.060	4786	8.2	growth line
QG1-7189-2	1.91	0.035	2.99	0.031	4869	8.7	

QG1-7246-1 (sampled 4/27/2009)

Sample ID	δ13C (VPDB)	δ13C ±	δ18O (VPDB)	δ18O ±	Distance (um)	T °C	comments
QG1-7246-1	0.23	0.047	3.38	0.101	172	7.1	
QG1-7246-1	-0.42	0.026	2.47	0.049	344	10.8	
QG1-7246-1	-0.59	0.024	2.50	0.044	516	10.7	
QG1-7246-1	-0.95	0.033	2.60	0.071	882	10.2	growth line
QG1-7246-1	-1.11	0.093	1.97	0.166	1076	12.9	
QG1-7246-1	-0.43	0.028	1.76	0.034	1270	13.7	
QG1-7246-1	-0.61	0.026	2.16	0.095	1437	12.1	
QG1-7246-1	-0.25	0.037	3.10	0.024	1604	8.2	
QG1-7246-1	-0.06	0.008	3.35	0.041	1771	7.2	growth line
QG1-7246-1	-0.22	0.069	3.33	0.099	1938	7.3	
QG1-7246-1	-0.86	0.039	2.62	0.079	2105	10.2	
QG1-7246-1	-0.74	0.023	2.08	0.081	2272	12.4	
QG1-7246-1	-0.38	0.040	2.39	0.023	2439	11.1	
QG1-7246-1	0.03	0.025	2.66	0.084	2606	10.0	
QG1-7246-1	0.30	0.016	3.49	0.046	2773	6.7	
QG1-7246-1	0.36	0.021	3.64	0.030	2940	6.1	growth line
QG1-7246-1	-0.64	0.025	2.35	0.020	3105	11.3	
QG1-7246-1	-0.34	0.007	2.34	0.014	3270	11.3	
QG1-7246-1	0.10	0.050	3.13	0.044	3435	8.1	
QG1-7246-1	-0.04	0.034	3.40	0.036	3600	7.0	growth line
QG1-7246-1	0.11	0.028	3.26	0.017	3765	7.6	
QG1-7246-1	-0.32	0.032	2.77	0.015	3930	9.6	
QG1-7246-1	-0.63	0.057	2.56	0.015	4095	10.4	
QG1-7246-1	-1.04	0.012	1.86	0.016	4260	13.4	
QG1-7246-1	-0.75	0.046	2.08	0.051	4417	12.4	
QG1-7246-1	-0.86	0.011	2.09	0.071	4574	12.4	
QG1-7246-1	-0.30	0.064	3.12	0.116	4731	8.2	growth line
QG1-7246-1	-0.46	0.025	3.02	0.040	4888	8.6	
QG1-7246-1	-1.22	0.005	2.12	0.016	5045	12.3	
QG1-7246-1	-0.59	0.018	2.57	0.026	5202	10.4	
QG1-7246-1	-0.17	0.072	3.13	0.105	5359	8.1	
QG1-7246-1	-0.05	0.010	3.52	0.039	5516	6.6	growth line
QG1-7246-1	-0.36	0.024	3.00	0.040	5673	8.6	
QG1-7246-1	-1.04	0.008	2.75	0.016	5830	9.7	
QG1-7246-1	-0.83	0.040	2.67	0.048	6016	10.0	
QG1-7246-1	-1.03	0.026	2.23	0.059	6202	11.8	
QG1-7246-1	-0.43	0.017	2.21	0.076	6388	11.9	
QG1-7246-1	-0.22		2.41		6574	11.0	
QG1-7246-1	0.21	0.028	3.45	0.033	6760	6.8	
QG1-7246-1	0.47	0.018	4.05	0.042	6946	4.5	growth line
QG1-7246-1	-0.26	0.049	3.24	0.108	7318	7.7	
QG1-7246-1	-0.77	0.044	2.39	0.021	7504	11.1	
QG1-7246-1	-0.18	0.037	2.41	0.024	7690	11.1	
QG1-7246-1	0.14	0.033	3.19	0.069	8074	7.9	
QG1-7246-1	0.22	0.023	3.17	0.045	8266	8.0	
QG1-7246-1	-0.12	0.035	2.54	0.063	8458	10.5	
QG1-7246-1	-0.15	0.058	2.14	0.017	8650	12.1	growth line
QG1-7246-1	0.23	0.055	2.01	0.016	8842	12.7	

QG1-7246-1	-0.10	0.018	2.65	0.027	9034	10.1	
QG1-7246-1	0.61	0.021	3.69	0.029	9226	5.9	growth line
QG1-7246-1	0.72	0.010	3.46	0.023	9394	6.8	
QG1-7246-1	0.34	0.018	3.05	0.080	9562	8.4	
QG1-7246-1	-0.15	0.011	2.13	0.075	9730	12.2	
QG1-7246-1	0.17	0.020	2.60	0.042	9898	10.3	
QG1-7246-1	0.09	0.057	2.81	0.135	10066	9.4	
QG1-7246-1	0.45	0.032	2.76	0.028	10234	9.6	
QG1-7246-1	1.03	0.072	3.59	0.038	10402	6.3	growth line
QG1-7246-1	0.58	0.050	3.07	0.022	10570	8.3	
QG1-7246-1	0.60	0.065	3.33	0.035	10738	7.3	
QG1-7246-1	0.97	0.013	2.93	0.021	11527	8.9	
QG1-7246-1	1.25	0.021	3.78	0.028	11707	5.6	growth line
QG1-7246-1	1.29	0.027	3.43	0.061	11887	6.9	
QG1-7246-1	1.20	0.056	3.31	0.031	12067	7.4	
QG1-7246-1	1.03	0.012	2.98	0.033	12247	8.7	
QG1-7246-1	0.96	0.050	2.57	0.014	12427	10.4	
QG1-7246-1	1.65	0.012	2.65	0.112	12607	10.1	
QG1-7246-1	1.91	0.011	2.11	0.049	12787	12.3	
QG1-7246-1	1.69	0.035	2.00	0.028	12967	12.7	
QG1-7246-1	1.05	0.041	1.88	0.090	13147	13.2	
QG1-7246-1	0.93	0.027	2.45	0.028	13327	10.9	
QG1-7246-1	0.83	0.041	2.95	0.092	13503	8.8	
QG1-7246-1	1.08	0.013	3.54	0.034	13679	6.5	growth line
QG1-7246-1	0.74	0.020	3.16	0.053	13855	8.0	
QG1-7246-1	0.21	0.035	2.41	0.020	14031	11.0	
QG1-7246-1	-0.18	0.016	1.90	0.086	14207	13.2	
QG1-7246-1	0.17	0.015	1.88	0.038	14383	13.2	
QG1-7246-1	0.00	0.040	2.46	0.024	14559	10.8	
QG1-7246-1	0.26	0.016	3.16	0.036	14735	8.0	growth line
QG1-7246-1	0.22	0.022	2.31	0.026	14911	11.5	
QG1-7246-1	0.54	0.056	2.38	0.075	15087	11.2	
QG1-7246-1	0.33	0.009	2.15	0.017	15439	12.1	

QG2-1061-1 (sampled 10/23/2008)

Sample ID	δ13C (VPDB)	δ13C ±	δ18O (VPDB)	δ18O ±	Distance (um)	T °C	comments
QG2-1061-1	0.92	0.065	2.66	0.059	0	10.0	growing edge
QG2-1061-1	0.88	0.027	3.74	0.037	148	5.7	growth line
QG2-1061-1	0.86	0.016	3.63	0.107	296	6.1	
QG2-1061-1	1.49	0.037	2.80	0.019	768	9.5	
QG2-1061-1	1.57	0.013	2.21	0.065	1254	11.9	
QG2-1061-1	1.57	0.032	2.18	0.055	1416	12.0	
QG2-1061-1	1.92	0.011	2.14	0.018	1578	12.2	
QG2-1061-1	1.80	0.010	2.07	0.055	1740	12.5	
QG2-1061-1	1.95	0.039	1.88	0.100	1902	13.3	
QG2-1061-1	2.05	0.134	1.97	0.016	2226	12.9	
QG2-1061-1	1.82	0.026	2.05	0.080	2388	12.5	
QG2-1061-1	1.44	0.011	2.00	0.070	2550	12.8	
QG2-1061-1	1.47	0.029	2.01	0.039	2874	12.7	
QG2-1061-1	1.44	0.050	2.35	0.013	3036	11.3	
QG2-1061-1	1.47	0.018	2.14	0.030	3424	12.2	
QG2-1061-1	1.45	0.014	2.55	0.076	3618	10.5	
QG2-1061-1	1.63	0.029	2.64	0.067	3812	10.1	

QG2-1061-1	1.52	0.053	2.73	0.054	4006	9.7	
QG2-1061-1	1.44	0.030	2.65	0.072	4200	10.1	
QG2-1061-1	1.60	0.008	2.72	0.029	4394	9.8	
QG2-1061-1	1.86	0.042	2.99	0.030	4588	8.7	
QG2-1061-1	1.69	0.010	2.93	0.040	4782	8.9	
QG2-1061-1	1.76	0.016	2.98	0.012	4976	8.7	
QG2-1061-1	1.39	0.045	2.92	0.044	5170	9.0	
QG2-1061-1	1.06	0.043	3.17	0.066	5364	8.0	
QG2-1061-1	1.02	0.035	3.48	0.014	5668	6.7	
QG2-1061-1	0.84	0.022	3.72	0.026	5820	5.8	
QG2-1061-1	0.80	0.025	3.66	0.065	5972	6.0	
QG2-1061-1	1.22	0.039	3.78	0.034	6124	5.6	growth line
QG2-1061-1	1.27	0.039	3.62	0.017	6276	6.2	
QG2-1061-1	1.08	0.007	3.34	0.031	6428	7.3	
QG2-1061-1	1.28	0.005	3.07	0.006	6580	8.4	
QG2-1061-1	1.35	0.011	2.73	0.012	6732	9.7	
QG2-1061-1	1.44	0.017	2.52	0.019	6884	10.6	
QG2-1061-1	1.35	0.021	2.39	0.046	7036	11.1	
QG2-1061-1	1.49	0.062	2.26	0.089	7188	11.7	
QG2-1061-1	1.62	0.017	2.31	0.095	7340	11.4	
QG2-1061-1	1.74	0.034	1.86	0.014	7644	13.3	
QG2-1061-1	1.85	0.025	1.50	0.108	7796	14.9	
QG2-1061-1	1.76	0.031	1.92	0.006	7978	13.1	
QG2-1061-1	1.71	0.034	1.83	0.038	8524	13.5	
QG2-1061-1	2.14	0.011	2.18	0.068	9252	12.0	
QG2-1061-1	1.91	0.017	1.83	0.033	9434	13.5	
QG2-1061-1	1.87	0.035	1.85	0.094	9616	13.4	
QG2-1061-1	1.73	0.074	1.90	0.097	9798	13.1	
QG2-1061-1	1.54	0.007	2.09	0.013	9980	12.4	
QG2-1061-1	1.60	0.053	2.05	0.011	10162	12.5	
QG2-1061-1	1.83	0.025	2.00	0.066	10344	12.7	
QG2-1061-1	1.79	0.017	1.84	0.006	10526	13.4	
QG2-1061-1	1.81	0.035	2.13	0.025	10702	12.2	
QG2-1061-1	1.94	0.102	2.11	0.035	10878	12.3	
QG2-1061-1	2.23	0.012	2.20	0.010	11054	11.9	
QG2-1061-1	2.05	0.031	2.34	0.084	11230	11.3	
QG2-1061-1	2.02	0.017	2.38	0.005	11406	11.2	
QG2-1061-1	1.73	0.023	2.18	0.058	11582	12.0	
QG2-1061-1	1.41	0.012	2.22	0.046	11758	11.8	
QG2-1061-1	1.45	0.023	2.71	0.021	11934	9.8	
QG2-1061-1	1.49	0.059	2.80	0.026	12252	9.4	
QG2-1061-1	1.40	0.009	3.05	0.081	12411	8.4	
QG2-1061-1	1.36	0.041	3.15	0.030	12729	8.0	
QG2-1061-1	1.43	0.033	3.71	0.022	12888	5.8	growth line
QG2-1061-1	1.47	0.025	3.56	0.031	13206	6.4	
QG2-1061-1	1.62	0.024	3.46	0.041	13365	6.8	
QG2-1061-1	2.05	0.014	3.47	0.098	13683	6.8	
QG2-1061-1	1.67	0.036	3.36	0.056	13842	7.2	
QG2-1061-1	1.69	0.027	3.36	0.019	14001	7.2	
QG2-1061-1	1.58	0.025	3.19	0.013	14319	7.9	
QG2-1061-1	1.69	0.049	3.06	0.067	14478	8.4	

QG2-1064-1 (sampled 9/18/2008)

Sample ID	δ13C (VPDB)	δ13C ±	δ18O (VPDB)	δ18O ±	Distance (um)	T °C	comments
QG2-1064-1	0.47	0.006	2.14	0.109	0	12.1	growing edge

QG2-1064-1	0.59	0.022	2.11	0.037	100	12.3	
QG2-1064-1	0.40	0.024	2.40	0.039	200	11.1	growth line
QG2-1064-1	0.16	0.018	2.21	0.013	300	11.9	
QG2-1064-1	0.23	0.010	2.32	0.049	400	11.4	
QG2-1064-1	0.47	0.047	2.44	0.077	500	10.9	
QG2-1064-1	0.82	0.009	2.85	0.013	600	9.2	growth line
QG2-1064-1	0.65	0.043	2.78	0.079	700	9.5	
QG2-1064-1	-0.10	0.027	2.27	0.025	800	11.6	
QG2-1064-1	-0.39	0.005	2.05	0.088	900	12.5	
QG2-1064-1	-0.60	0.057	2.04	0.107	1000	12.6	
QG2-1064-1	-0.66	0.046	1.95	0.031	1100	13.0	
QG2-1064-1	0.09	0.012	2.14	0.093	1200	12.2	
QG2-1064-1	0.64	0.031	2.84	0.073	1494	9.3	growth line
QG2-1064-1	0.04	0.033	2.57	0.091	1788	10.4	
QG2-1064-1	-0.62	0.032	2.26	0.016	1935	11.6	
QG2-1064-1	-0.66	0.008	2.07	0.017	2075	12.4	
QG2-1064-1	-0.67	0.016	1.82	0.031	2215	13.5	
QG2-1064-1	-0.41	0.033	1.90	0.078	2355	13.2	
QG2-1064-1	-0.14	0.010	1.89	0.019	2495	13.2	
QG2-1064-1	0.40	0.011	1.92	0.026	2635	13.1	
QG2-1064-1	0.48	0.009	2.22	0.043	2775	11.8	
QG2-1064-1	0.43	0.035	2.33	0.050	2915	11.4	
QG2-1064-1	0.77	0.021	2.83	0.041	3017	9.3	
QG2-1064-1	0.96	0.017	3.00	0.067	3119	8.7	
QG2-1064-1	1.09	0.048	3.31	0.062	3221	7.4	
QG2-1064-1	1.07	0.024	3.25	0.030	3323	7.6	
QG2-1064-1	1.21	0.050	3.59	0.011	3425	6.3	
QG2-1064-1	0.72	0.151	3.64	0.083	3629	6.1	growth line
QG2-1064-1	0.44	0.038	3.25	0.048	3731	7.6	
QG2-1064-1	0.40	0.019	3.11	0.025	3833	8.2	
QG2-1064-1	-0.18	0.028	2.69	0.046	4139	9.9	
QG2-1064-1	-0.05	0.009	2.56	0.047	4241	10.4	
QG2-1064-1	-0.03	0.066	2.40	0.095	4343	11.1	
QG2-1064-1	-0.08	0.012	2.37	0.067	4445	11.2	
QG2-1064-1	0.18	0.026	2.31	0.040	4560	11.5	
QG2-1064-1	0.29	0.013	1.93	0.085	4675	13.1	
QG2-1064-1	0.64	0.045	2.05	0.053	4790	12.5	
QG2-1064-1	0.57	0.025	2.05	0.053	5020	12.5	
QG2-1064-1	0.70	0.027	2.01	0.083	5135	12.7	
QG2-1064-1	0.91	0.050	2.00	0.070	5250	12.7	
QG2-1064-1	0.89	0.040	2.20	0.040	5365	11.9	
QG2-1064-1	1.01	0.060	2.30	0.023	5480	11.5	
QG2-1064-1	1.06	0.021	2.28	0.054	5595	11.6	
QG2-1064-1	1.20	0.036	2.39	0.057	5710	11.1	
QG2-1064-1	1.22	0.024	2.58	0.058	5825	10.3	
QG2-1064-1	1.15	0.017	2.45	0.067	6055	10.9	
QG2-1064-1	0.83	0.035	2.55	0.082	6170	10.5	
QG2-1064-1	1.08	0.074	2.79	0.119	6400	9.5	
QG2-1064-1	1.17	0.037	3.06	0.024	6540	8.4	
QG2-1064-1	1.10	0.033	3.35	0.026	6680	7.3	
QG2-1064-1	1.20	0.022	3.40	0.096	6820	7.1	
QG2-1064-1	1.07	0.013	3.40	0.056	6960	7.0	
QG2-1064-1	0.93	0.017	3.72	0.090	7100	5.8	growth line
QG2-1064-1	0.82	0.024	3.25	0.052	7240	7.6	
QG2-1064-1	0.83	0.078	3.18	0.026	7380	7.9	
QG2-1064-1	0.58	0.065	2.90	0.065	7520	9.1	

QG2-1064-1	0.23	0.048	2.71	0.065	7660	9.8	
QG2-1064-1	0.23	0.024	2.75	0.018	7800	9.7	
QG2-1064-1	-0.10	0.034	2.25	0.088	7940	11.7	
QG2-1064-1	-0.32	0.035	2.14	0.030	8080	12.2	
QG2-1064-1	-0.42	0.029	2.47	0.012	8220	10.8	
QG2-1064-1	-0.49	0.011	1.95	0.026	8500	12.9	
QG2-1064-1	-0.03	0.046	2.23	0.041	8640	11.8	
QG2-1064-1	0.04	0.037	2.16	0.017	8773	12.1	
QG2-1064-1	0.71	0.017	1.97	0.040	9039	12.9	
QG2-1064-1	1.17	0.025	1.98	0.050	9172	12.9	
QG2-1064-1	0.78	0.011	1.84	0.040	9305	13.4	
QG2-1064-1	1.08	0.016	1.95	0.047	9438	12.9	
QG2-1064-1	1.67	0.019	2.17	0.097	9571	12.1	
QG2-1064-1	1.21	0.047	2.19	0.076	9704	11.9	
QG2-1064-1	1.47	0.074	2.65	0.042	9970	10.1	
QG2-1064-1	0.56	0.035	3.17	0.040	10236	8.0	
QG2-1064-1	0.73	0.058	3.29	0.051	10369	7.5	
QG2-1064-1	-1.34	0.031	-0.40	0.050	10502	23.4	
QG2-1064-1	0.36	0.034	3.48	0.031	10768	6.7	
QG2-1064-1	0.31	0.093	3.50	0.087	10901	6.6	
QG2-1064-1	0.64	0.010	3.59	0.040	11175	6.3	growth line
QG2-1064-1	1.00	0.008	2.86	0.024	11312	9.2	
QG2-1064-1	0.32	0.005	2.60	0.045	11449	10.2	
QG2-1064-1	0.27	0.028	2.27	0.101	11586	11.6	
QG2-1064-1	-0.06	0.028	2.21	0.080	11723	11.9	
QG2-1064-1	0.04	0.022	2.10	0.032	11860	12.3	
QG2-1064-1	0.36	0.032	1.97	0.031	11997	12.9	
QG2-1064-1	0.48	0.053	1.88	0.028	12134	13.2	
QG2-1064-1	0.83	0.007	1.91	0.093	12271	13.1	
QG2-1064-1	1.14	0.036	2.85	0.021	12408	9.3	
QG2-1064-1	1.36	0.054	2.43	0.017	12545	11.0	
QG2-1064-1	1.30	0.023	2.40	0.054	12682	11.1	
QG2-1064-1	1.18	0.061	2.26	0.078	12819	11.7	

QG2-7180-1 (sampled 10/16/2008)

Sample ID	δ13C (VPDB)	δ13C ±	δ18O (VPDB)	δ18O ±	Distance (um)	T °C	comments
QG2-7180-1	0.96	0.081	3.44	0.089	104	6.9	growth line
QG2-7180-1	0.55	0.031	3.26	0.039	208	7.6	
QG2-7180-1	0.54	0.012	1.97	0.127	541	12.9	
QG2-7180-1	0.72	0.063	2.01	0.058	652	12.7	
QG2-7180-1	0.63	0.032	1.90	0.017	874	13.2	
QG2-7180-1	0.44	0.032	1.74	0.080	985	13.9	
QG2-7180-1	0.42	0.024	1.91	0.019	1096	13.1	
QG2-7180-1	0.59	0.063	2.09		1318	12.4	
QG2-7180-1	-0.03	0.060	1.99	0.073	1540	12.8	
QG2-7180-1	-0.22	0.044	2.19	0.075	1762	11.9	
QG2-7180-1	-0.41	0.068	2.33	0.020	1873	11.4	
QG2-7180-1	-0.14	0.032	2.89	0.039	2127	9.1	
QG2-7180-1	0.14	0.038	3.35	0.050	2270	7.2	
QG2-7180-1	0.29	0.027	3.95	0.053	2413	4.9	growth line
QG2-7180-1	-0.67	0.010	2.29	0.026	2842	11.5	
QG2-7180-1	-0.54	0.042	2.23	0.062	2985	11.8	
QG2-7180-1	0.01	0.051	2.01	0.024	3128	12.7	

QG2-7180-1	0.98		2.20		3271	11.9	
QG2-7180-1	0.92	0.015	2.02	0.107	3414	12.7	
QG2-7180-1	0.68	0.017	2.10	0.049	3557	12.3	
QG2-7180-1	0.22	0.040	1.86	0.033	3700	13.3	
QG2-7180-1	0.76	0.041	2.65	0.076	4314	10.1	
QG2-7180-1	0.70	0.029	2.82	0.105	4970	9.4	
QG2-7180-1	0.79	0.082	3.16	0.021	5134	8.0	
QG2-7180-1	0.62	0.051	3.67	0.041	6282	6.0	growth line
QG2-7180-1	0.29	0.028	2.64	0.100	6610	10.1	
QG2-7180-1	0.90	0.045	2.45	0.020	7266	10.9	
QG2-7180-1	1.45	0.059	1.85	0.033	7759	13.4	
QG2-7180-1	1.26	0.057	1.79	0.053	7924	13.6	
QG2-7180-1	1.33	0.016	1.81	0.103	8089	13.6	
QG2-7180-1	1.67	0.010	2.14	0.104	8254	12.1	
QG2-7180-1	1.50	0.014	2.09	0.026	8419	12.4	
QG2-7180-1	1.60	0.019	2.13	0.050	8749	12.2	
QG2-7180-1	1.53	0.035	2.18	0.096	8914	12.0	
QG2-7180-1	1.64	0.035	2.16	0.056	9079	12.1	
QG2-7180-1	1.44	0.010	2.08	0.040	9244	12.4	
QG2-7180-1	1.18	0.009	2.30	0.081	9409	11.5	
QG2-7180-1	1.14	0.029	2.43	0.076	9574	11.0	
QG2-7180-1	0.95	0.028	2.40	0.045	9739	11.1	
QG2-7180-1	0.75	0.013	2.61	0.070	9904	10.2	
QG2-7180-1	0.67	0.040	2.61	0.016	10069	10.2	
QG2-7180-1	0.63	0.027	2.71	0.050	10234	9.8	
QG2-7180-1	0.82	0.025	3.14	0.032	10399	8.1	
QG2-7180-1	0.88	0.037	2.90	0.106	10564	9.0	
QG2-7180-1	0.71	0.038	3.15	0.014	10729	8.0	
QG2-7180-1	0.53	0.053	3.27	0.052	10894	7.6	
QG2-7180-1	0.86	0.049	3.41	0.092	11059	7.0	
QG2-7180-1	1.17	0.021	3.54	0.015	11224	6.5	growth line
QG2-7180-1	1.19	0.019	3.36	0.072	11389	7.2	
QG2-7180-1	0.89	0.010	2.75	0.062	11554	9.7	
QG2-7180-1	1.07	0.007	2.63	0.059	11734	10.1	
QG2-7180-1	0.99	0.002	2.58	0.010	11914	10.4	
QG2-7180-1	0.90	0.015	2.61	0.052	12094	10.2	
QG2-7180-1	0.88	0.042	2.46	0.006	12274	10.8	
QG2-7180-1	0.74	0.032	2.28	0.042	12454	11.6	
QG2-7180-1	0.56	0.005	2.07	0.080	12634	12.5	
QG2-7180-1	1.00	0.014	2.03	0.075	12814	12.6	
QG2-7180-1	0.72	0.020	1.73	0.058	12994	13.9	
QG2-7180-1	0.57	0.037	1.71	0.054	13174	14.0	
QG2-7180-1	0.83	0.062	1.94	0.054	13354	13.0	
QG2-7180-1	0.74	0.066	1.79	0.045	13534	13.6	
QG2-7180-1	0.73	0.023	1.66	0.021	13714	14.2	
QG2-7180-1	0.75	0.013	1.55	0.005	13894	14.7	
QG2-7180-1	0.65	0.020	1.61	0.036	14074	14.4	
QG2-7180-1	0.57	0.041	1.70	0.024	14254	14.0	
QG2-7180-1	0.64	0.035	1.75	0.040	14434	13.8	
QG2-7180-1	0.88	0.016	1.81	0.087	14614	13.6	
QG2-7180-1	0.97	0.005	1.86	0.096	14794	13.3	
QG2-7180-1	1.14	0.034	2.01	0.030	14974	12.7	
QG2-7180-1	1.16	0.035	1.88	0.031	15154	13.3	

QG2-7180-2 (sampled 4/22/2009)

Sample ID	δ13C (VPDB)	δ13C ±	δ18O (VPDB)	δ18O ±	Distance (um)	T °C	comments
QG2-7180-2	2.38	0.026	2.60	0.078	912	10.3	
QG2-7180-2	2.42	0.038	2.49	0.077	1092	10.7	
QG2-7180-2	2.68	0.013	2.74	0.060	1272	9.7	growth line
QG2-7180-2	2.76	0.080	2.65	0.089	1452	10.1	
QG2-7180-2	2.47	0.015	2.53	0.070	1632	10.5	
QG2-7180-2	2.46	0.011	2.55	0.014	1812	10.5	
QG2-7180-2	2.09	0.026	2.32	0.049	1992	11.4	
QG2-7180-2	2.27	0.027	2.97	0.097	2172	8.8	
QG2-7180-2	2.23	0.016	3.27	0.040	2352	7.5	
QG2-7180-2	2.51	0.025	3.62	0.020	2532	6.2	
QG2-7180-2	2.31	0.041	3.58	0.090	2712	6.3	
QG2-7180-2	2.35	0.014	3.86	0.059	2892	5.2	growth line
QG2-7180-2	1.77	0.019	3.34	0.029	3072	7.3	
QG2-7180-2	1.92	0.023	3.33	0.052	3252	7.3	
QG2-7180-2	1.94	0.043	3.52	0.040	3432	6.6	
QG2-7180-2	1.73	0.008	3.61	0.040	3792	6.2	
QG2-7180-2	2.17	0.005	4.04	0.053	3972	4.6	
QG2-7180-2	2.34	0.055	4.18	0.102	4152	4.0	growth line
QG2-7180-2	2.15	0.062	3.20	0.024	4332	7.8	
QG2-7180-2	2.27	0.076	2.67	0.060	4530	10.0	
QG2-7180-2	2.20	0.018	2.52	0.062	4926	10.6	
QG2-7180-2	2.26	0.059	2.07	0.098	5130	12.5	
QG2-7180-2	2.24	0.004	1.84	0.043	5334	13.4	
QG2-7180-2	2.32	0.045	1.91	0.023	5544	13.1	
QG2-7180-2	2.83	0.022	2.12	0.041	5754	12.3	
QG2-7180-2	2.79	0.019	2.08	0.016	5964	12.4	
QG2-7180-2	2.52	0.010	1.96	0.061	6174	12.9	
QG2-7180-2	2.17	0.034	1.74	0.017	6384	13.9	
QG2-7180-2	2.55	0.027	2.17	0.018	6594	12.0	
QG2-7180-2	2.29	0.017	1.89	0.029	6804	13.2	
QG2-7180-2	2.49	0.029	1.82	0.047	7012	13.5	
QG2-7180-2	2.59	0.039	1.84	0.065	7220	13.4	
QG2-7180-2	2.76	0.028	1.85	0.051	7636	13.4	
QG2-7180-2	2.70	0.050	1.64	0.023	7844	14.3	
QG2-7180-2	2.85	0.026	1.95	0.052	8052	12.9	
QG2-7180-2	2.90	0.020	2.03	0.048	8260	12.6	
QG2-7180-2	3.01	0.061	2.07	0.045	8468	12.4	
QG2-7180-2	2.85	0.039	2.22	0.066	8884	11.8	growth line
QG2-7180-2	2.55	0.010	1.96	0.014	9092	12.9	
QG2-7180-2	2.28	0.051	1.85	0.017	9287	13.4	
QG2-7180-2	2.38	0.033	1.65	0.109	9482	14.2	
QG2-7180-2	2.76	0.017	2.12	0.030	9677	12.2	
QG2-7180-2	2.79	0.013	2.31	0.014	9872	11.5	
QG2-7180-2	2.73	0.039	2.13	0.027	10067	12.2	
QG2-7180-2	2.81	0.029	3.01	0.077	10457	8.6	growth line
QG2-7180-2	2.32	0.003	2.82	0.072	10847	9.4	
QG2-7180-2	1.81	0.026	2.40	0.016	11042	11.1	
QG2-7180-2	2.05	0.058	2.94	0.051	11237	8.9	
QG2-7180-2	1.55	0.006	2.93	0.063	11632	8.9	
QG2-7180-2	1.92	0.018	3.13	0.018	11832	8.1	
QG2-7180-2	1.80	0.038	3.26	0.037	12032	7.6	
QG2-7180-2	2.21	0.032	3.80	0.005	12232	5.5	growth line

QG2-7180-2	2.14	0.023	3.21	0.093	12632	7.8
QG2-7180-2	2.32	0.061	3.63	0.079	12832	6.1
QG2-7180-2	2.34	0.014	3.49	0.032	13032	6.7
QG2-7180-2	2.45	0.080	3.57	0.100	13432	6.4
QG2-7180-2	2.29	0.017	3.08	0.056	13632	8.3
QG2-7180-2	2.28	0.031	2.88	0.083	13832	9.1
QG2-7180-2	2.03	0.024	2.65	0.075	14032	10.1
QG2-7180-2	1.95	0.040	2.37	0.153	14232	11.2
QG2-7180-2	1.84	0.021	2.55	0.016	14432	10.4
QG2-7180-2	2.11	0.005	2.95	0.052	14633	8.8
QG2-7180-2	1.64	0.011	2.35	0.042	15035	11.3
QG2-7180-2	1.78	0.048	2.41	0.026	15437	11.0
QG2-7180-2	1.65	0.022	1.96	0.081	15638	12.9
QG2-7180-2	1.67	0.003	2.22	0.076	16040	11.8
QG2-7180-2	1.85	0.018	2.53	0.054	16241	10.6
QG2-7180-2	2.05	0.018	2.41	0.024	16442	11.0
QG2-7180-2	2.07	0.049	2.38	0.102	16664	11.2
QG2-7180-2	1.99	0.038	2.28	0.112	17108	11.6
QG2-7180-2	2.03	0.038	2.17	0.083	17330	12.0
QG2-7180-2	1.87	0.017	1.91	0.037	17552	13.1
QG2-7180-2	2.19	0.008	2.31	0.010	17774	11.4
QG2-7180-2	1.97	0.038	1.90	0.050	17996	13.2
QG2-7180-2	2.49	0.060	2.07	0.094	18218	12.5
QG2-7180-2	2.31	0.040	1.86	0.032	18440	13.3
QG2-7180-2	2.38	0.033	2.07	0.046	18662	12.5

ORK-LT-5 (sampled 4/20/2009)

Sample ID	δ13C (VPDB)	δ13C ±	δ18O (VPDB)	δ18O ±	Distance (um)	T °C	comments
ORK-LT-5	-0.50	0.032	0.80	0.061	0	17.9	growing edge
ORK-LT-5	-0.84	0.013	2.18	0.099	172	12.0	
ORK-LT-5	-0.72	0.043	2.26	0.051	344	11.6	
ORK-LT-5	-0.03	0.090	3.33	0.010	688	7.3	
ORK-LT-5	0.34	0.020	3.55	0.060	851	6.5	
ORK-LT-5	0.29	0.035	2.80	0.053	1014	9.4	
ORK-LT-5	0.08	0.015	2.23	0.011	1177	11.8	
ORK-LT-5	0.08	0.008	2.19	0.043	1340	11.9	
ORK-LT-5	-0.17	0.018	2.06	0.058	1503	12.5	
ORK-LT-5	-0.12	0.041	2.09	0.036	1666	12.4	
ORK-LT-5	-0.23	0.023	2.69	0.076	1992	9.9	
ORK-LT-5	-0.14	0.032	3.19	0.065	2155	7.9	
ORK-LT-5	-0.05	0.016	3.57	0.025	2318	6.4	
ORK-LT-5	0.14	0.053	3.68	0.049	2481	6.0	
ORK-LT-5	-0.12	0.001	2.90	0.026	2644	9.1	
ORK-LT-5	-0.29	0.033	2.34	0.031	2839	11.3	
ORK-LT-5	-0.46	0.012	1.91	0.089	3034	13.1	
ORK-LT-5	-0.25	0.049	1.77	0.048	3229	13.7	
ORK-LT-5	-0.03	0.020	3.35	0.065	3424	7.2	
ORK-LT-5	0.26	0.176	3.57	0.212	3619	6.4	
ORK-LT-5	0.00	0.062	2.93	0.023	3814	8.9	
ORK-LT-5	0.08	0.057	2.35	0.111	4009	11.3	

APPENDIX B: NOAA SST reconstruction 1961-2009

Date	Temp (°C)
1-Jan-61	7.95
1-Feb-61	6.90
1-Mar-61	7.43
1-Apr-61	8.02
1-May-61	8.85
1-Jun-61	10.28
1-Jul-61	11.18
1-Aug-61	11.98
1-Sep-61	11.20
1-Oct-61	10.55
1-Nov-61	9.86
1-Dec-61	9.11
1-Jan-62	8.27
1-Feb-62	7.90
1-Mar-62	7.66
1-Apr-62	8.25
1-May-62	9.51
1-Jun-62	10.62
1-Jul-62	11.50
1-Aug-62	12.18
1-Sep-62	11.58
1-Oct-62	10.87
1-Nov-62	9.98
1-Dec-62	9.22
1-Jan-63	8.49
1-Feb-63	8.17
1-Mar-63	8.19
1-Apr-63	8.23
1-May-63	8.99
1-Jun-63	10.22
1-Jul-63	11.37
1-Aug-63	11.56
1-Sep-63	11.69
1-Oct-63	10.92
1-Nov-63	9.94
1-Dec-63	9.43
1-Jan-64	8.70
1-Feb-64	8.24
1-Mar-64	8.33
1-Apr-64	8.15
1-May-64	9.13
1-Jun-64	10.25
1-Jul-64	11.88
1-Aug-64	12.38
1-Sep-64	11.71
1-Oct-64	10.66
1-Nov-64	10.19
1-Dec-64	9.31
1-Jan-65	8.52
1-Feb-65	8.06
1-Mar-65	8.10
1-Apr-65	8.91
1-May-65	9.66
1-Jun-65	10.95
1-Jul-65	11.72
1-Aug-65	12.36
1-Sep-65	12.11
1-Oct-65	11.22
1-Nov-65	10.04
1-Dec-65	9.12
1-Jan-66	8.46
1-Feb-66	8.13
1-Mar-66	7.93
1-Apr-66	8.23
1-May-66	9.09
1-Jun-66	10.61
1-Jul-66	11.79
1-Aug-66	12.47
1-Sep-66	11.97
1-Oct-66	11.06
1-Nov-66	10.18
1-Dec-66	9.52
1-Jan-67	8.63
1-Feb-67	8.18
1-Mar-67	7.80
1-Apr-67	7.28
1-May-67	8.15
1-Jun-67	9.60
1-Jul-67	11.31
1-Aug-67	11.93
1-Sep-67	11.63
1-Oct-67	10.90
1-Nov-67	10.28
1-Dec-67	9.45
1-Jan-68	8.62
1-Feb-68	8.07
1-Mar-68	7.79
1-Apr-68	8.08
1-May-68	9.17
1-Jun-68	11.06
1-Jul-68	12.60
1-Aug-68	12.90

Date	Temp (°C)
1-Sep-68	12.23
1-Oct-68	11.12
1-Nov-68	10.58
1-Dec-68	9.27
1-Jan-69	8.59
1-Feb-69	8.11
1-Mar-69	8.01
1-Apr-69	8.22
1-May-69	8.99
1-Jun-69	10.10
1-Jul-69	11.17
1-Aug-69	12.25
1-Sep-69	11.92
1-Oct-69	11.14
1-Nov-69	10.31
1-Dec-69	9.36
1-Jan-70	8.57
1-Feb-70	8.35
1-Mar-70	7.56
1-Apr-70	7.79
1-May-70	8.65
1-Jun-70	10.06
1-Jul-70	11.73
1-Aug-70	12.92
1-Sep-70	12.69
1-Oct-70	11.50
1-Nov-70	10.10
1-Dec-70	8.79
1-Jan-71	8.05
1-Feb-71	7.83
1-Mar-71	7.82
1-Apr-71	8.31
1-May-71	9.25
1-Jun-71	10.72
1-Jul-71	12.01
1-Aug-71	12.62
1-Sep-71	12.21
1-Oct-71	10.75
1-Nov-71	9.89
1-Dec-71	9.00
1-Jan-72	8.23
1-Feb-72	7.79
1-Mar-72	7.79
1-Apr-72	8.15
1-May-72	9.41
1-Jun-72	10.83
1-Jul-72	12.12
1-Aug-72	12.77
1-Sep-72	12.68
1-Oct-72	11.12
1-Nov-72	10.23
1-Dec-72	9.37
1-Jan-73	8.35
1-Feb-73	7.99
1-Mar-73	7.94
1-Apr-73	8.18
1-May-73	9.28
1-Jun-73	10.64
1-Jul-73	12.26
1-Aug-73	12.39
1-Sep-73	12.23
1-Oct-73	11.10
1-Nov-73	10.06
1-Dec-73	9.54
1-Jan-74	8.79
1-Feb-74	8.20
1-Mar-74	8.59
1-Apr-74	8.85
1-May-74	9.52
1-Jun-74	10.71
1-Jul-74	11.82
1-Aug-74	12.01
1-Sep-74	11.47
1-Oct-74	10.21
1-Nov-74	9.57
1-Dec-74	9.11
1-Jan-75	8.08
1-Feb-75	8.42
1-Mar-75	7.73
1-Apr-75	7.77
1-May-75	8.77
1-Jun-75	10.40
1-Jul-75	12.23
1-Aug-75	12.75
1-Sep-75	12.22
1-Oct-75	11.11
1-Nov-75	9.61
1-Dec-75	9.25
1-Jan-76	8.73
1-Feb-76	8.03
1-Mar-76	7.53
1-Apr-76	8.00
1-May-76	9.57
1-Jun-76	10.58
1-Jul-76	11.77
1-Aug-76	12.19
1-Sep-76	11.55
1-Oct-76	11.71
1-Nov-76	10.04
1-Dec-76	9.45

Date	Temp (°C)
1-Jan-77	8.96
1-Feb-77	8.53
1-Mar-77	8.39
1-Apr-77	8.38
1-May-77	9.39
1-Jun-77	10.32
1-Jul-77	11.70
1-Aug-77	12.28
1-Sep-77	11.67
1-Oct-77	10.76
1-Nov-77	10.36
1-Dec-77	9.02
1-Jan-78	8.00
1-Feb-78	8.43
1-Mar-78	8.28
1-Apr-78	8.25
1-May-78	9.30
1-Jun-78	9.97
1-Jul-78	11.86
1-Aug-78	12.77
1-Sep-78	12.16
1-Oct-78	10.65
1-Nov-78	10.43
1-Dec-78	9.83
1-Jan-79	8.68
1-Feb-79	7.69
1-Mar-79	7.37
1-Apr-79	8.04
1-May-79	8.73
1-Jun-79	10.09
1-Jul-79	11.64
1-Aug-79	12.35
1-Sep-79	11.57
1-Oct-79	10.70
1-Nov-79	10.05
1-Dec-79	8.73
1-Jan-80	8.17
1-Feb-80	8.20
1-Mar-80	8.71
1-Apr-80	8.57
1-May-80	9.28
1-Jun-80	10.40
1-Jul-80	12.29
1-Aug-80	13.50
1-Sep-80	12.78
1-Oct-80	11.28
1-Nov-80	10.06
1-Dec-80	9.51
1-Jan-81	8.51
1-Feb-81	8.41
1-Mar-81	7.42
1-Apr-81	7.81
1-May-81	9.07
1-Jun-81	10.02
1-Jul-81	11.67
1-Aug-81	12.17
1-Sep-81	12.34
1-Oct-81	11.26
1-Nov-81	10.15
1-Dec-81	9.76
1-Jan-82	8.97
1-Feb-82	8.43
1-Mar-82	8.13
1-Apr-82	8.62
1-May-82	9.32
1-Jun-82	10.73
1-Jul-82	12.75
1-Aug-82	12.92
1-Sep-82	11.92
1-Oct-82	11.00
1-Nov-82	9.91
1-Dec-82	9.06
1-Jan-83	8.94
1-Feb-83	8.57
1-Mar-83	8.33
1-Apr-83	8.38
1-May-83	9.26
1-Jun-83	10.49
1-Jul-83	11.76
1-Aug-83	12.49
1-Sep-83	12.29
1-Oct-83	11.13
1-Nov-83	10.23
1-Dec-83	9.02
1-Jan-84	8.95
1-Feb-84	8.74
1-Mar-84	8.25
1-Apr-84	7.63
1-May-84	8.64
1-Jun-84	10.32
1-Jul-84	11.91
1-Aug-84	12.66
1-Sep-84	12.63
1-Oct-84	10.98
1-Nov-84	10.54
1-Dec-84	9.46
1-Jan-85	8.59
1-Feb-85	8.39
1-Mar-85	7.25
1-Apr-85	7.66

Date	Temp (ºC)
1-May-85	8.49
1-Jun-85	9.80
1-Jul-85	10.97
1-Aug-85	11.21
1-Sep-85	11.75
1-Oct-85	10.58
1-Nov-85	9.52
1-Dec-85	9.11
1-Jan-86	8.16
1-Feb-86	7.27
1-Mar-86	6.58
1-Apr-86	7.54
1-May-86	8.46
1-Jun-86	9.41
1-Jul-86	11.29
1-Aug-86	12.13
1-Sep-86	12.10
1-Oct-86	11.15
1-Nov-86	10.21
1-Dec-86	9.54
1-Jan-87	9.00
1-Feb-87	8.30
1-Mar-87	7.74
1-Apr-87	8.12
1-May-87	8.29
Jan-91	8.42
Feb-91	7.65
Mar-91	7.51
Apr-91	7.84
May-91	8.52
Jun-91	9.89
Jul-91	12.88
Aug-91	13.68
Sep-91	12.92
Oct-91	11.38
Nov-91	10.24
Dec-91	9.22
Jan-92	8.46
Feb-92	7.98
Mar-92	7.70
Apr-92	7.51
May-92	9.00
Jun-92	11.37
Jul-92	12.52
Aug-92	12.70
Sep-92	11.90
Oct-92	11.03
Nov-92	9.83
Dec-92	8.83
Jan-93	8.05
Feb-93	7.64
Mar-93	7.37
Apr-93	7.69
May-93	8.67
Jun-93	9.65
Jul-93	10.81
Aug-93	11.51
Sep-93	11.41
Oct-93	10.40
Nov-93	9.56
Dec-93	8.39
Jan-94	7.27
Feb-94	6.52
Mar-94	6.25
Apr-94	6.87
May-94	8.16
Jun-94	9.70
Jul-94	11.87
Aug-94	12.74
Sep-94	12.04
Oct-94	11.03
Nov-94	10.48
Dec-94	9.36
Jan-95	7.97
Feb-95	7.41
Mar-95	7.04
Apr-95	7.18
May-95	8.23
Jun-95	9.98
Jul-95	12.17
Aug-95	13.91
Sep-95	12.92
Oct-95	11.63
Nov-95	10.63
Dec-95	9.68
Jan-96	8.38
Feb-96	7.68
Mar-96	7.03
Apr-96	7.22
May-96	8.07
Jun-96	9.85
Jul-96	11.53
Aug-96	12.91
Sep-96	12.71
Oct-96	11.58
Nov-96	10.40
Dec-96	8.92
Jan-97	8.09
Feb-97	7.70
Mar-97	7.63

Date	Temp (ºC)
Apr-97	7.97
May-97	8.85
Jun-97	10.56
Jul-97	12.58
Aug-97	14.26
Sep-97	12.63
Oct-97	12.12
Nov-97	11.42
Dec-97	10.37
Jan-98	9.43
Feb-98	8.68
Mar-98	8.48
Apr-98	8.24
May-98	9.41
Jun-98	10.30
Jul-98	11.56
Aug-98	12.28
Sep-98	12.39
Oct-98	11.28
Nov-98	10.12
Dec-98	9.14
Jan-99	8.31
Feb-99	7.50
Mar-99	7.27
Apr-99	7.85
May-99	8.96
Jun-99	9.95
Jul-99	12.29
Aug-99	12.98
Sep-99	12.57
Oct-99	11.65
Nov-99	10.74
Dec-99	9.05
Jan-00	7.94
Feb-00	7.64
Mar-00	7.73
Apr-00	7.49
May-00	9.55
Jun-00	10.29
Jul-00	11.47
Aug-00	12.94
Sep-00	12.37
Oct-00	11.48
Nov-00	10.37
Dec-00	9.71
Jan-01	8.89
Feb-01	7.49
Mar-01	7.05
Apr-01	7.30
May-01	9.00

Date	Temp (ºC)
Jun-01	10.15
Jul-01	11.89
Aug-01	12.95
Sep-01	12.26
Oct-01	11.99
Nov-01	10.84
Dec-01	9.59
Jan-02	8.57
Feb-02	8.30
Mar-02	7.69
Apr-02	8.11
May-02	9.34
Jun-02	11.73
Jul-02	12.89
Aug-02	13.97
Sep-02	13.34
Oct-02	12.31
Nov-02	10.80
Dec-02	10.08
Jan-03	9.03
Feb-03	8.12
Mar-03	7.93
Apr-03	8.57
May-03	9.57
Jun-03	11.82
Jul-03	13.60
Aug-03	14.42
Sep-03	13.41
Oct-03	11.95
Nov-03	11.18
Dec-03	10.17
Jan-04	9.02
Feb-04	8.30
Mar-04	8.06
Apr-04	8.19
May-04	9.26
Jun-04	11.07
Jul-04	12.57
Aug-04	14.02
Sep-04	12.96
Oct-04	11.71
Nov-04	11.12
Dec-04	10.02
Jan-05	8.55
Feb-05	7.90
Mar-05	7.54
Apr-05	7.96
May-05	8.73
Jun-05	10.51
Jul-05	12.81

Date	Temp (ºC)
Aug-05	12.75
Sep-05	12.37
Oct-05	11.80
Nov-05	11.22
Dec-05	9.95
Jan-06	8.95
Feb-06	8.34
Mar-06	7.47
Apr-06	7.51
May-06	8.57
Jun-06	10.67
Jul-06	13.07
Aug-06	13.56
Sep-06	13.29
Oct-06	12.50
Nov-06	11.18
Dec-06	10.11
Jan-07	9.00
Feb-07	8.31
Mar-07	8.15
Apr-07	8.49
May-07	9.45
Jun-07	11.13
Jul-07	12.46
Aug-07	12.46
Sep-07	11.83
Oct-07	11.39
Nov-07	10.46
Dec-07	9.32
Jan-08	8.45
Feb-08	7.84
Mar-08	7.48
Apr-08	7.67
May-08	9.94
Jun-08	11.26
Jul-08	12.15
Aug-08	13.52
Sep-08	13.04
Oct-08	11.66
Nov-08	10.41
Dec-08	9.06
Jan-09	8.23
Feb-09	7.72
Mar-09	7.73
Apr-09	8.25
May-09	9.39
Jun-09	11.73
Jul-09	14.11
Aug-09	14.12
Sep-09	13.07